

Synthesis of zinc titanate for Dye Sensitized Solar Cell (DSSC) application

by

Azman bin Azumi

10368

Dissertation submitted in partial fulfillment of
the requirements for the
Bachelor of Engineering (Hons)
(Chemical Engineering)

Supervisor : Assoc. Prof. Dr. Anita Ramli.

Jan 2010

Universiti Teknologi PETRONAS
Bandar Seri Iskandar
31750 Tronoh
Perak Darul Ridzuan

CERTIFICATION OF APPROVAL

Synthesis of zinc titanate for Dye Sensitized Solar Cell (DSSC) application

By

Azman bin Azumi

A project dissertation submitted to Chemical Engineering Program

Universiti Teknologi Petronas

in partial fulfillment of the requirements for the

Bachelor of Engineering (Hons)

(Chemical Engineering)

Approved by:

Assoc. Prof. Dr. Anita Ramli

UNIVERSITI TEKNOLOGI PETRONAS

TRONOH, PERAK

JUNE 2010

CERTIFICATION OF ORIGINALITY

This is to certify that I am responsible for the work submitted in this project, that the original work is my own except as specified in the references and acknowledgements, and that the original work contained herein have not been undertaken or done by unspecified sources or persons.

AZMAN BIN AZUMI

ABSTRACT

The objectives of the project are to synthesis zinc titanate and characterize the structure for Dye Sensitized Solar Cells (DCCS) application. The porous structure of zinc titanate will increase the light absorption at the longer wavelength of sunlight and increase the efficiency of the DSSC system.

Currently, intensive research was done by researcher to increase the efficiency of DSSCs system so that it can be used in industrial scale. There are many factors that effect the efficiency of DSSCs system and one of it is the characteristic of electrode used. The parameters such the surface area, porosity, crystalline grains, and rate of recombination of photoinduced electron are important in determining the efficiency of DSSCs system.

In this project, zinc titanate will be synthesis by two methods that are reflux and impregnation method. The composition of the reactant will be varies to prepare different sample of zinc titanate. The characteristic zinc titanate structure will be tested to identify the best compositon in producing zinc titanate that can be applied in DSSC system. The zinc titanate produced will be tested by using x-ray diffusion (XRD), FTIR, UV-vis, scanning electron microscopy (SEM), and BET analysis. After that, the sample of zinc titanate will be tested in the test cells to determine the electricity generation.

Most of the researcher found that the most favorable temperature to synthesis zinc titanate is between 800°C to 945°C. The amount of zinc also needs to be less than titanium to keep the efficiency of DSSCs system high.

ACKNOWLEDGEMENT

First and foremost, thank to God for His blessing and mercy in completing this one year project. It would befit to extend my outstretched gratitude to Assoc. Professor Dr. Anita Ramli, Fundamental and Applied Sciences Department, Universiti Teknologi Petronas. It is a privilege to be under her supervision. Even with her tight schedules as Head of Department and high commitment to Universiti Teknologi Petronas, there was no moment where she fails to provide support and guidance. Her advices and moral support gave a sense of strength and confidence in conducting the final year project.

Many thank to our Final Year Project Coordinators, for their unlimited contributions success in providing the students with guidelines and seminars to enlighten hopes of confidence. Not forget to thank all lab executive and technicians as their willingness to provide the facilities and entertain our demand during conducting the project.

Last but not least, thank to all the Universiti Teknologi Petronas involved lecturers and students who have been contributing great efforts and ideas making this final year project a success.

TABLE OF CONTENTS

ABSTRACT	iii
TABLE OF CONTENTS.....	vi
CHAPTER 1: INTRODUCTION	1
CHAPTER 2: LITERATURE REVIEW AND THEORY	4
CHAPTER 3: METHODOLOGY	12
CHAPTER 4: RESULTS AND DISCUSSION.....	18
CHAPTER 5: CONCLUSION AND RECOMMENDATION	26
REFERENCES	27
APPENDICES.....	29

LIST OF FIGURES

Figure 1.1: The flow of electron in DSSC system.....	1
Figure 2.1: XRD and SEM result for hydrothermal and reflux.....	7
Figure 2.2: Dependence of crystal structure and thermal stability.....	8
Figure 2.3: Diffuse reflectance UV-vis spectra.....	8
Figure 2.4: ZnO-TiO ₂ phase diagram.....	10
Figure 2.5: XRD profiles of ZnTiO ₃ powders	11
Figure 2.6: Crystallinity of ZnTiO ₃	11
Figure 3.1: Project Process Flow	12
Figure 3.2: Milestone for FYP I	14
Figure 3.3: Milestone for FYP II	15
Figure 4.1 : Tauc plot comparison for all samples.....	18
Figure 4.2 : Absorbance of the samples.....	18
Figure 4.3: 1:1 mol ratio Zn-TiO ₂	20
Figure 4.4: 1:2 mol ratio Zn-TiO ₂	20
Figure 4.5: 2:1 mol ratio Zn-TiO ₂	20
Figure 4.6: 5 wt% Zn-TiO ₂	20
Figure 4.7: 10 wt% Zn-TiO ₂	21
Figure 4.8: 15 wt% Zn-TiO ₂	21
Figure 4.9: Impregnation before calcine.....	22
Figure 4.10: Impregnation after calcine.....	22
Figure 4.11: Reflux before calcine.....	23
Figure 4.12: Reflux after calcine.....	23
Figure 4.13: XRD result for reflux sample.....	24
Figure 4.14: XRD result for impregnation sample.....	24

LIST OF TABLES

Table 4.1: Band gap energy of zinc titanate.....	19
---	----

CHAPTER 1

INTRODUCTION

1.1 Background of study

Solar cell is a device that converts the light into electrical energy in photovoltaic energy conversion. However the high cost of solar cell has remained a limiting factor for the implementation of solar electricity in a large scale. Recently, the general trend of nanotechnology emerged in the field of photovoltaic energy conversion. Development of material in nanometer scale has generated new photovoltaic materials and systems that could potentially lead to realization of low-cost solar cells in the future. The most well known photovoltaic system is the dye-sensitized nanostructured solar cell (DSSC) developed by Grätzel (Grätzel 1991).

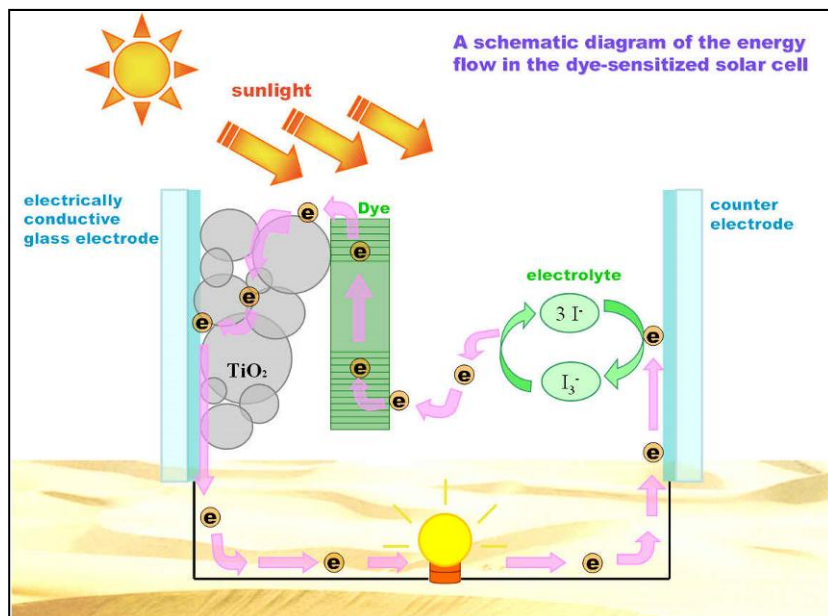


Figure 1.1: The flow of electron in DSSC system

When the DSSC is illuminated with sunlight, the dye will absorb the light and becomes excited. The excited dye inject electron to the conduction band of semiconductor. At the same time, the oxidize dye is reduced by electron donor and returns to ground state. The electrons in the conduction band are collected at the counter electrode and flow through the external circuit.

1.2 Problem statement

The solar spectrum has a large photon flux in the wavelength region 500–1,000 nm, and a good overlap of the optical absorption spectrum of the sensitizer with the solar spectrum is helpful to achieve higher performance of the DSSC. To enhance light absorption or extending the spectral response to the wavelength, employing light scattering structures such as some metal oxide particles with several hundred nanometers in diameter or admixture of some larger particles to increase the average optical path length of the light within the film. Employing these scattering structures will enhance photocurrent by increasing the light absorption at longer wavelength region ($600 < \lambda < 800$ nm).

Currently, the highest efficiency electrode in DSSC system is titanium dioxide (TiO_2). However, this electrode only caters for visible light that have wavelength range from 400nm to 700nm. By hybridization of TiO_2 and ZnO , it will produce more spacious band gap. The wide gap provides more porous structure and space for the light absorption to occur as it not only caters for visible light, but also the diffuse light.

ZnO is selected because of the properties of that structure that have electron mobility higher than TiO_2 . Even though the band gap of TiO_2 and ZnO is very similar, TiO_2 have indirect band gap and ZnO have direct band gap. It has high exciton binding energy 60meV, and gives a higher resistance for thermally induce exciton recombination (Soga, 2006, p.231).

1.3 Objectives

- To synthesis zinc titanate by using impregnation and reflux method
- To characterize the zinc titanate.
- To determine the best composition ratio that gives the optimum structure of the zinc titanate nanocrystal.
- To determine the efficiency of the zinc titanate nanostructure in DSSCs system.

1.4 Scope of study

This research project is carried out to synthesis zinc titanate that will provide more porous structure of nanohybrid electrode. The parameters that will be study in this research are the method to synthesis zinc titanate and the effects of composition.

The zinc titanate produced then will be characterized by using x-ray diffusion (XRD), UV-vis analysis, FTIR, surface area analysis by using BET technique, and scanning electron microscope (SEM). After that, the zinc titanate will be integrated into a test cell to determine the effect of the sample in electricity generation. The amount of electricity generated will be compared to determine the best method and composition that increase the efficiency of DSSCs system as compare to TiO₂ electrode only.

This project is relevant enough as it cover on the preparation of the zinc titanate nanostructured material, characterization of sample produced and sample performance test. This project is feasible as it can be done within the time frame if there is no delay on chemical order and equipment failure.

CHAPTER 2

LITERATURE REVIEW

DSSC technology gives a large flexibility in the choice of the components allowing the ability to fine-tune the properties of the solar cell. The choice of metal oxide for the nanostructures electrode will affect the range of band gap, band edge positions, the density of states and the electron transport and loss properties. The choice will also affect the possibility to obtain different shapes and doping densities of the nanoparticles. For each choice of oxide material the particle size, the surface structure and the porosity and film thickness are also important parameters to optimize for each type of sensitizing dye and redox system.

At present, nanostructure TiO₂ was used as the electrode for DSSC system. The electrode has huge surface area per projected area that can drastically increase effective light absorption. The current highest energy conversion efficiency is over 11% and it's possible to increase the efficiency of this DSSC by manipulating the structure of electrode (Soga, 2006, p.193).

Hua Yu et al. (2009) has synthesis TiO₂ organic sol for the preparation of a compact TiO₂ layer on fluorine-doped tin oxide (FTO) glass by a dip-coating technique. The resultant thin film was used for the fabrication of DSSCs. The compact layer typically has a thickness of ca. 110 nm as indicated by its SEM, and consists of anatase as confirmed by the XRD pattern. Compared with the traditional DSSCs without this compact layer, the solar energy-to-electricity conversion efficiency, short-circuit current and open-circuit potential of the DSSCs with the compact layer were improved by 33.3%, 20.3%, and 10.2%, respectively. This can be attributed to the merits brought by the compact layer. It can effectively improve adherence of TiO₂ to FTO surface, provide a larger TiO₂/FTO contact area, and reduce the electron recombination by blocking the direct contact between the redox electrolyte and the conductive FTO surface.

Yanan Fu and co-worker have synthesized TiO₂ synthesized by sol–gel route using poly (alkylene oxide) block copolymer as template and tetrabutyl orthotitanate as titanium source. They investigate the influence of acetylacetone (AcAc), glacial acetic acid, HCl and AcAc-HCl as inhibitors on hydrolysis/condensation reaction. The mesopore structure, crystalline phase and optical characteristics were analyzed by N₂ adsorption, X-ray diffraction, transmission electron microscopy and UV–VIS–NIR spectrum. Photoaction measurements were performed on dye-sensitized solar cells (DSSCs) using the mesoporous TiO₂ as photoanodes. They found that the formed films are anatase phase and mesoporous structure. Different restraining mechanisms of these inhibitors to hydrolysis/condensation process lead to different mesoporous structure whose specific surface area (BET) varies from 34 to 176 m²/g, and crystal size is from 5.6 to 38.2 nm. The mesoporous photoanode with high BET and large crystalline grains will increase the conversion efficiency of the DSSCs system.

Seok-Soon Kim and co-researcher examined the method for preparing a flexible dye-sensitized solar cell for commercial competitiveness of a DSSC and fabricate a newphotoelectrode using ZnO coated TiO₂ nanoparticles to provide an inherent energy barrier at the electrode/electrolyte interface leading to a reduced recombination of photoinduced electrons. The cell performance was compared through I–V curve and wavelength dependent photocurrent measurements of the two types of DSSC. The value of short-circuit current density, voltage, fill factor, and overall conversion efficiency increased from 0.35 to 0.49 mA/cm², from –0.67 to –0.72V, from 61.1 to 69.0%, and from 0.71 to 1.21%, respectively without any post-treatments.

Mingdeng Wei et al. (2006) found a high light-to-electricity conversion efficiency of 10% by applying mesoporous TiO₂ as an electrode material. This high efficiency can be attributed to thenovel physicochemical properties of mesoporous TiO₂, which include high surface area, uniform nanochannels and a homogeneous nanocrystalline TiO₂ several nm in size arranged along the framework. The high surface area allows adsorption of a large volume of dye, resulting in a higher photocurrent density.

ZnO also is an attractive material that can be used as electrode as it has wide-band gap semiconductor with good carrier mobility. The electron mobility in ZnO is much higher than TiO₂. However, the chemical stability of ZnO is less than TiO₂ that can cause problems in the dye adsorption procedure. The efficiency of ZnO solar cells so far significantly lower than TiO₂ which is 4-5% (Soga, 2006, p.227-228). ZnO nanomaterials are expected to form energy barriers at the electrode-electrolyte interface because the conduction band edge of ZnO (100 mV) is more negative than that of TiO₂ (B.Posters et al. 2008).

Sang Pang et al. (2007) has conducted a research on the effect of ZnO nanorodes on the efficiency of TiO₂ DSSC system. They found that the solar conversion efficiency of the DSSCs after the addition of ZnO nanorods (1 wt %) was increased by about 15% compared to that without ZnO nanorods. They highlight that first, charge effective diffusion and the suppression of recombination are the origin for the enhancement of voltage and fill factor; second, the shift of the conduction band edge position in the TiO₂/ZnO electrodes is proposed as the main cause of the enhancement of voltage.

K. E. Kim and co-researcher (2007) found that ZnO-covered TiO₂ film electrode enables enhancement of short-circuit photocurrent density, open-circuit voltage and consequently solar conversion efficiency for a DSSCs by 12%, 17%. And 23% respectively, compared to those of bare TiO₂ electrode system.

J.H. Hyung et al. (2009) found that covered TiO₂ electrodes with ZnO nanowire will improve the photovoltaic properties of DSSCs or in other word, increase the efficiency of the system. The ZnO nanowires were grown on the surface of a TiO₂ thin-film electrode with zinc dehydrate acetate seeds by using thermal chemical vapor deposition. The covered electrode improved the open-circuit voltage and the fill factor while significantly decreasing the short-circuit current density and photovoltaic performance of the covered electrode compared to bare TiO₂ electrode. The current and fill factor of the covered electrode were enhanced by about 10-15% compared with bare TiO₂ electrode system.

Tae Woo Kim and co-workers have synthesized mesoporous nanohybrids interstratified with zinc oxide nanoparticles and layered titanate nanosheets by exfoliation-restacking method. They also found that the lattice stability of the resulting nanohybrids could be greatly enhanced by hydrothermal treatment. The fitting analysis based on BET equation gives $\text{ZnO}-\text{Ti}_{1.83}\text{O}_4$ by hydrothermal treatment and its calcined derivatives expanded surface areas of 114 and $119-134 \text{ m}^2\text{g}^{-1}$ respectively. The structures properties of $\text{ZnO}-\text{Ti}_{1.83}\text{O}_4$ were characterized by x-ray diffusion (XRD). The result for XRD analysis is tabulated in Figure 1.

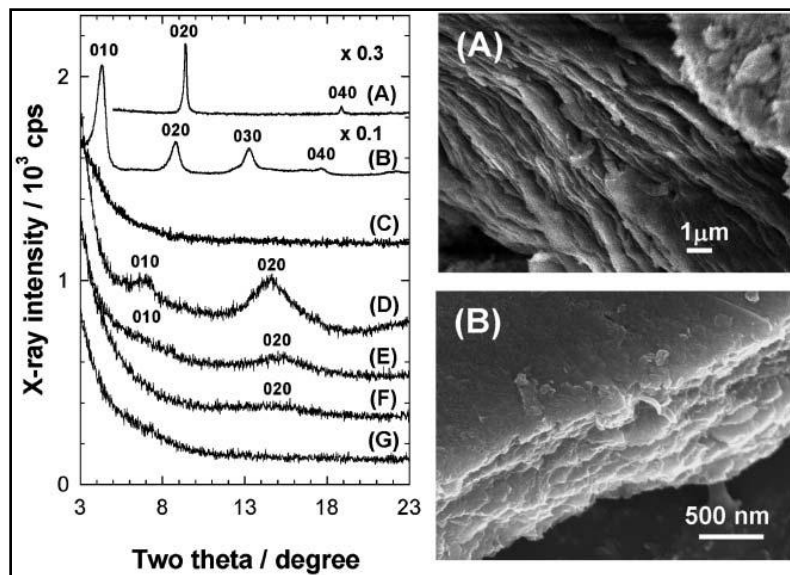


Figure 2.1: Left panel: small angle XRD patterns of (A) the protonic titanate, (B) $\text{ZnO}-\text{Ti}_{1.83}\text{O}_4$ by reflux treatment and (C) its derivative calcined at 200 uC , (D) $\text{ZnO}-\text{Ti}_{1.83}\text{O}_4$ by hydrothermal treatment and its derivatives calcined at (E) 200 , (F) 300 , and (G) 400 uC . Each pattern is shifted along the y-axis for clarity. Right panel: FE-SEM (field emission scanning electron microscopy) images of (A) $\text{ZnO}-\text{Ti}_{1.83}\text{O}_4$ by reflux treatment and (B) $\text{ZnO}-\text{Ti}_{1.83}\text{O}_4$ hydrothermal treatment.

After heat-treatment at 200°C , $\text{ZnO}-\text{Ti}_{1.83}\text{O}_4$ by reflux treatment shows complete disappearance of (010) reflections indicate that the disintercalation of the guest species and the formation of ZnO on the sample surface. On the other hand, the calcined derivative $\text{ZnO}-\text{Ti}_{1.83}\text{O}_4$ by hydrothermal treatment at 200°C retain series of (010) reflections without the appearance of ZnO peaks. The heat-treatment at 400°C can completely remove (010) peaks as well as to the development of weak ZnO peaks at high angle region.

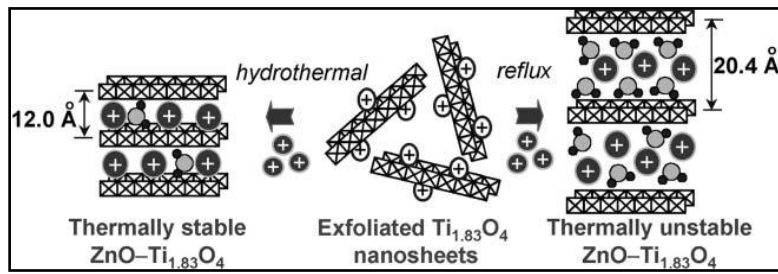


Figure 2.2: Dependence of crystal structure and thermal stability of porous zinc oxide-layered titanate nanohybrids on the synthetic conditions.

From the least squares fitting analysis, they find that the basal spacing is 20.4 \AA for the zinc titanate by reflux treatment and 20.0 \AA by hydrothermal treatment. This finding prove that the effectiveness of hydrothermal method in improving the heterostructure stability.

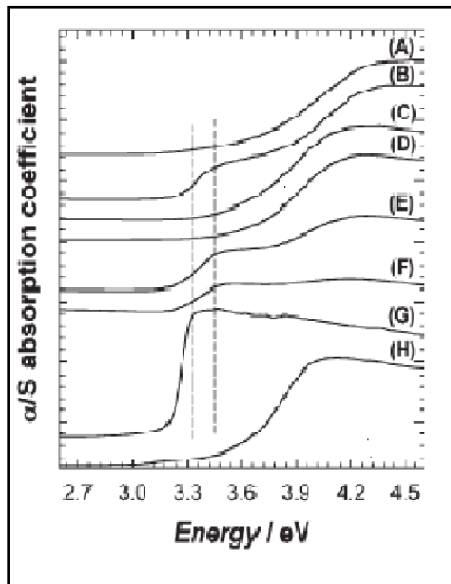


Figure 2.3: Diffuse reflectance UV-vis spectra of (A) ZnO-Ti1.83O4-R and (B) its derivative calcined at 200 uC, (C) ZnO-Ti1.83O4-H and its derivatives calcined at (D) 200, (E) 300, and (F) 400 uC, together with the reference spectra of (G) ZnO and (H) Cs0.67Ti1.83O4. Each spectrum is shifted along the y-axis for clarity. The dashed lines are guidelines for easier interpretation of the figure.

UV-vis analysis gives the zinc titanate nanohybrids 3.6-3.7 eV that are greater than ZnO (3.2 eV) due to the quantum confinement effect of hybridized ZnO species. During calcinations, at 200°C, no detectable change occurs in the UV-vis spectrum of ZnO-Ti_{1.83}O₄ by hydrothermal treatment, while calcined derivative by reflux treatment shows appearance of a new absorption edge at ~ 3.3 eV; indicate the formation of ZnO on the sample surface.

N. Labus and co-researchers are using the most common way for obtaining metatitanate $ZnTiO_3$ that is the sol-gel method. This method provides fine and homogeneous $ZnTiO_3$ particles with a high specific surface area. Because of the diffusion path is reduced, the temperature needed for synthesis in the subsequent treatment is lowered. The low temperature is required for the formation of $ZnTiO_3$ because of the decomposition of $ZnTiO_3$ to Zn_2TiO_4 and rutile at $945^\circ C$.

Yamaguchi et al. (1987) clarified that $Zn_2Ti_3O_8$ is a low-temperature form of $ZnTiO_3$. Zn_2TiO_4 can easily be prepared by conventional solid-state reaction between 2 ZnO and 1 TiO_2 . But, the preparation of pure $ZnTiO_3$ from mixture of 1 ZnO and 1 TiO_2 has not been successful because the compound decomposes into Zn_2TiO_4 and rutile at about $945^\circ C$ as mentioned above by N. Labus et al (2005).

Chang et al. (2002) highlight that the properties of materials depend on their synthesis processes, for $ZnTiO_3$, its physical-chemical properties are influenced by the synthesizing conditions. The solid-state reaction method has some drawbacks of high temperature, large particle size and limited degree of chemical homogeneity. In contrast, the chemical solution methods such as sol-gel method can provide products of fine and homogeneous particles with high specific surface area. The Pechini method is a conventional approach to prepare powder consisting of oxides of transition element. They prepared $ZnTiO_3$ powders by sol-gel method by using zinc acetate, ethylene glycol, titanium butoxide, and citric acid anhydrous and found that the crystallinity of $ZnTiO_3$ powders increase with increasing calcinations temperature and times, and the best conditions for calcinations is $800^\circ C$ for 10 hours. The morphology of $ZnTiO_3$ powders formed fiber type when calcinations temperature increased to $1000^\circ C$ and the grain size from the research were about 20 to 40nm.

J.Yang and J.H. Swisher has conducted a research to study the phase stability of Zn_2TiO_8 . Several types of experiments were carried out to obtain additional information on $ZnO-TiO_2$ phase diagram and they found that $Zn_2Ti_3O_8$ is a thermodynamically stable compound up to a temperature of $800^\circ C$. Above than that, it will transform sequentially into $ZnTiO_3$ and then into Zn_2TiO_4 . The new $ZnO-TiO_2$ phase diagram is shown in Figure 5 as comparison to the previous phase diagram introduced by Dulin and Rase in 1960.

Chai et al. (2007) has study the effects of heat treatment on the structure of zinc titanate prepared by Pechini process. The steps involve in heating process including dehydration reaction, decomposition, combustion reaction and zinc titanate formation. The crystallinity of zinc titanate have been improved by increasing the calcinations temperature. The optimum temperature for calcinations is at 800°C for 6 hours. The microstructures of zinc titanate have been validated using transmission electron microscopy (TEM) and the grain sizes are shown to vary between 20nm and 50nm. The x-ray diffusion (XRD) profiles with different calcinations temperature are shown in Figure 6 and the crystallinity of zinc titanate with respect to temperature is shown in Figure 7. Both of the figures prove that the best temperature to synthesis zinc titanate is at 800°C.

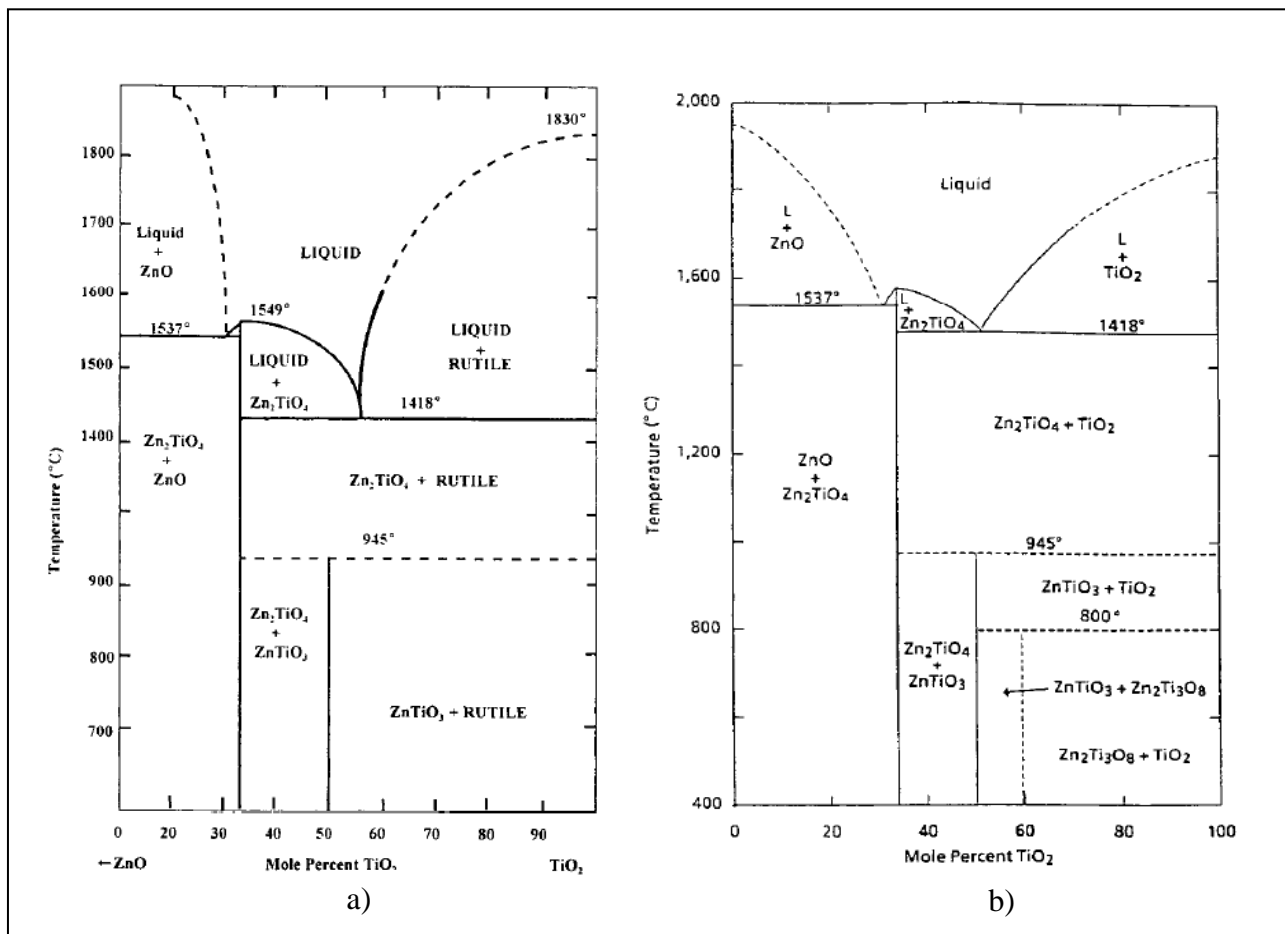


Figure 2.4: a) ZnO-TiO₂ phase diagram published by Dulin and Rase in 1960, b) Proposed new ZnO-TiO₂ phase diagram by J.Yang and J.H. Swisher in1996.

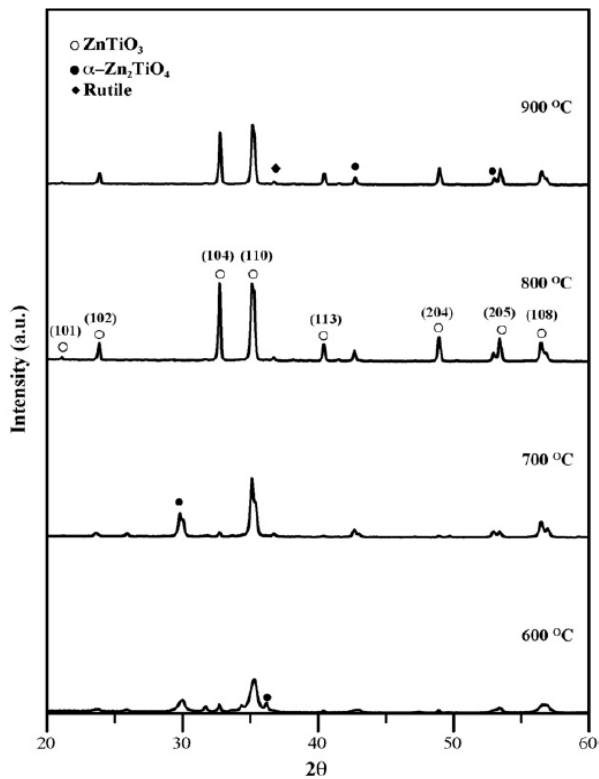


Figure 2.5: XRD profiles of ZnTiO₃ powders derived from ZnTiO₃ precursor solution after heat-treatment at different temperatures for 6 hours.

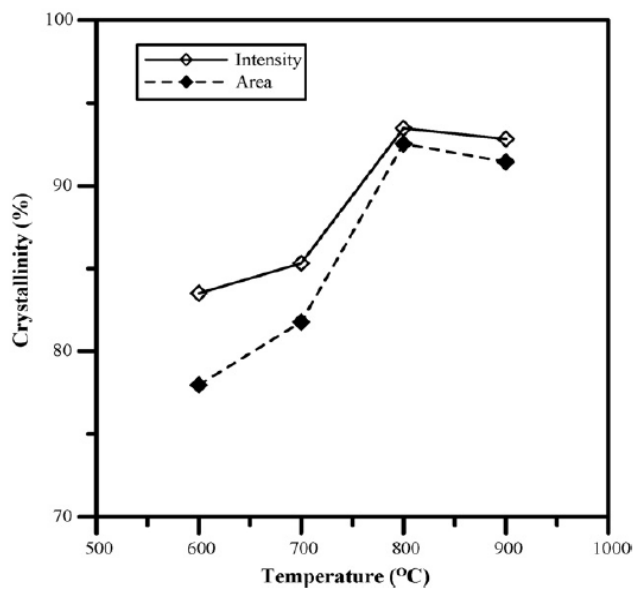


Figure 2.6: Crystallinity of ZnTiO₃ precursor solution after heat-treated at various temperatures for 6 hours.

CHAPTER 3

METHODOLOGY

3.1 Project Flow

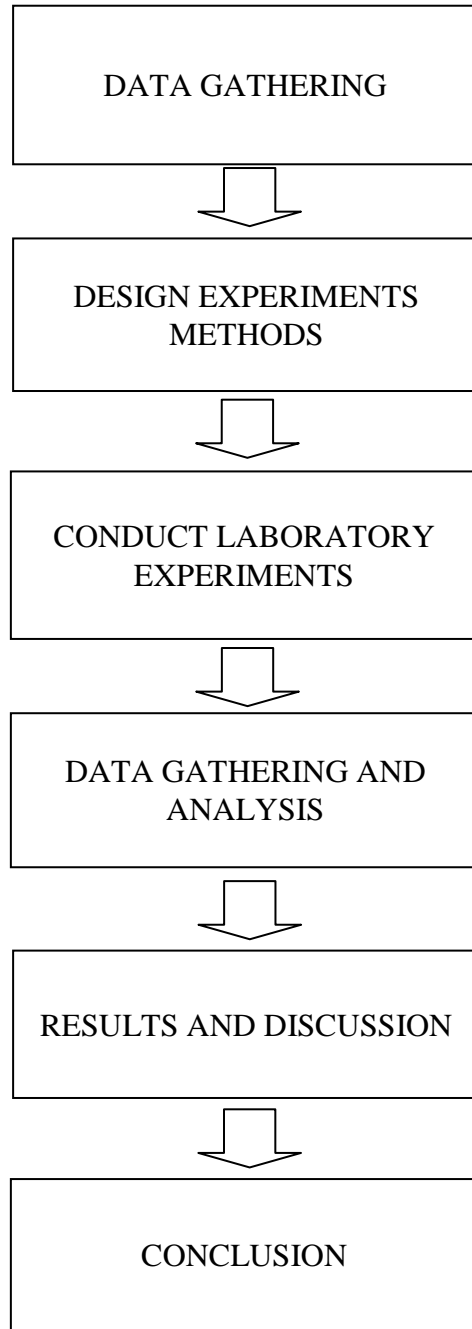


Figure 3.1: Project Process Flow

3.2 Sample preparation

Method 1: Reflux treatment

Zinc titanate was prepared by first dissolving 1 mol of zinc nitrate with distilled water in a beaker and adds 1 mol of titanium oxide into the solution. The mixture is then stirred for 30 minutes to get well distribution of titanium dioxide in the solution. After that, the mixture is reflux for 5 hours by using heating mantel at its boiling point temperature. Then, transfer the mixture from one-neck flask into a beaker and put it in the drying oven for 120°C overnight. The purpose of drying sample at 120°C is to make sure that all the water is vaporized and removed from the sample. Next, is to calcine the samples in the furnace for 5 hours at 500°C to remove the entire nitrate group in the samples. The experiment was repeated for 2 to 1 and 1 to 2 mol ratio of zinc to titanium.

Method 2: Impregnation

For the second method in getting zinc titanate, weight about 5% of zinc from the final weight (approximately 14.5g zinc nitrate for 100g sample). The solution is then added with remaining 95% titanium dioxide. After that, the mixture is stirred for 5 hours by using magnetic stirrer at 500 rpm. Then, the sample is dried in the drying oven at 120°C for one night. Next, the sample is calcine in the furnace at temperature 500°C for 5 hours as to remove the entire nitrate group in the mixture. The experiment was repeated for 10% and 15% amount of zinc in the sample.

3.2 Milestone for Final Year Project (FYP) I

Phases	Detail/Week	1	2	3	4	5	6	7	8	9	10	11	12	13	14
1	Selection of Project Topic														
	Proposal Submission														
	Approval on Proposal														
	Identification of chemicals														
2	Check Availability of Apparatus														
3	Submission of Preliminary Report														
4	Seminar 1														
5	Experiment Methodology Identification														
	Finalize Experimental Methodology														
6	Chemical Assesment and Hazard Identification														
7	Submission of Progress Report														
8	Seminar 2														
9	Submission of Interim Report														
10	Oral Presentation														

Figure 3.2: Milestone for FYP I

3.3 Milestone for Final Year Project (FYP) II

Phases	Detail/Week	1	2	3	4	5	6	7	8	9	10	11	12	13	14
1	Project Work Continue														
2	Submission of Progress Report 1														
3	Project Work Continue														
4	Submission of Progress Report 2														
5	Seminar														
6	Project Work Continue														
7	Poster Presentation														
8	Submission of Dissertation														

Figure 3.3: Milestone for FYP II

3.4 Characterization

XRD analysis

X-ray scattering techniques are reveal information about the crystallographic structure, chemical composition, and physical properties of materials and thin films. These techniques are based on observing the scattered intensity of an X-ray beam hitting a sample as a function of incident and scattered angle, polarization, and wavelength or energy. X-ray diffraction finds the geometry or shape of a molecule using X-rays. X-ray diffraction techniques are based on the elastic scattering of X-rays from structures that have long range order. For diffraction applications, only short wavelength x-rays (hard x-rays) in the range of a few angstroms to 0.1 angstrom (1 keV - 120 keV) are used. Because the wavelength of x-rays is comparable to the size of atoms, they are ideally suited for probing the structural arrangement of atoms and molecules in a wide range of materials. The energetic x-rays can penetrate deep into the materials and provide information about the bulk structure. The wave nature of the X-Rays diffracted by the lattice of the crystal to give a unique pattern of peaks of 'reflections' at differing angles and of different intensity, just as light can be diffracted by a grating of suitably spaced lines. The diffracted beams from atoms in successive planes cancel unless they are in phase, and the condition for this is given by the Bragg relationship;

$$n\lambda = 2d \sin \Theta$$

Where,

λ is the wavelength of the X-Rays

d is the distance between different plane of atoms in the crystal lattice.

Θ is the angle of diffraction.

Uv-vis analysis

Ultraviolet-visible spectroscopy or ultraviolet-visible spectrophotometry (UV-Vis or UV/Vis) involves the spectroscopy of photons in the UV-visible region. This means it uses light in the visible and adjacent (near ultraviolet (UV) and near infrared (NIR)) ranges. The absorption in the visible ranges directly affects the color of the chemicals involved. In this region of the electromagnetic spectrum, molecules undergo electronic transitions. This technique is complementary to fluorescence spectroscopy, in that fluorescence deals with transitions from the excited state to the ground state, while absorption measures transitions from the ground state to the excited state.

Scanning electron microscope (SEM) analysis

SEM is a type of electron microscope that images the sample surface by scanning it with a high-energy beam of electrons in a raster scan pattern. The electrons interact with the atoms that make up the sample producing signals that contain information about the sample's surface topography, composition and other properties such as electrical conductivity. The types of signals produced by an SEM include secondary electrons, back-scattered electrons (BSE), characteristic X-rays, specimen current and transmitted electrons.

FTIR

Fourier transform infrared (FTIR) spectroscopy is a measurement technique for collecting infrared spectra. Instead of recording the amount of energy absorbed when the frequency of the infra-red light is varied (monochromator), the IR light is guided through an interferometer. After passing through the sample, the measured signal is the interferogram. Performing a Fourier transform on this signal data results in a spectrum identical to that from conventional (dispersive) infrared spectroscopy.

CHAPTER 4

RESULTS AND DISCUSSION

4.1 Catalyst characterization

4.1.1 Diffuse Reflectance UV-Vis (DRS)

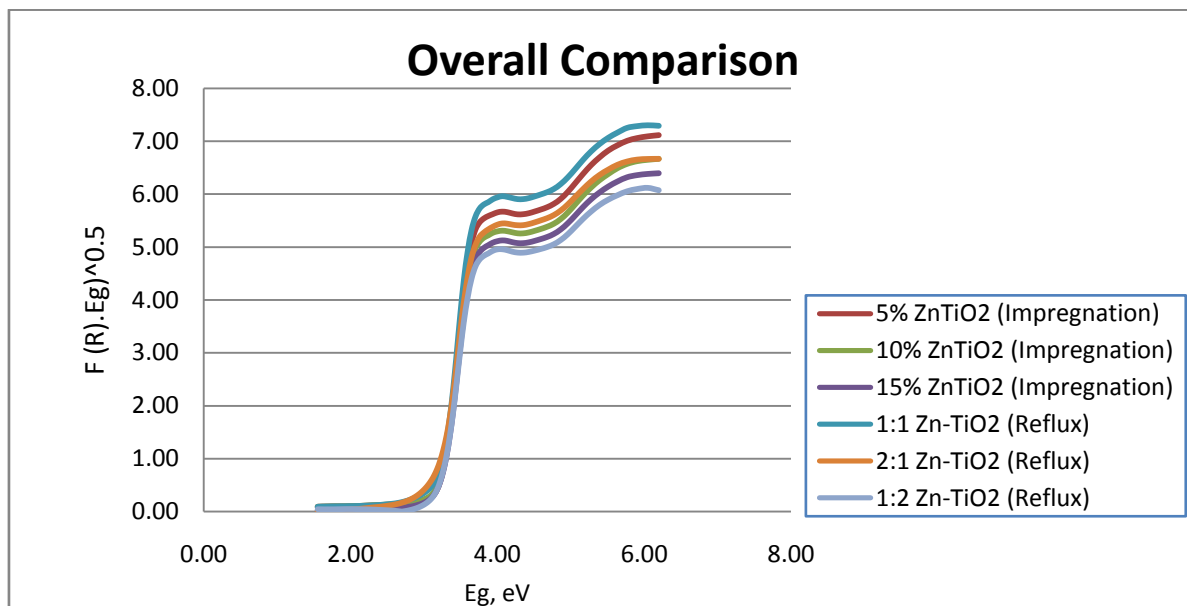


Figure 4.1 : Tauc plot comparison for all samples.

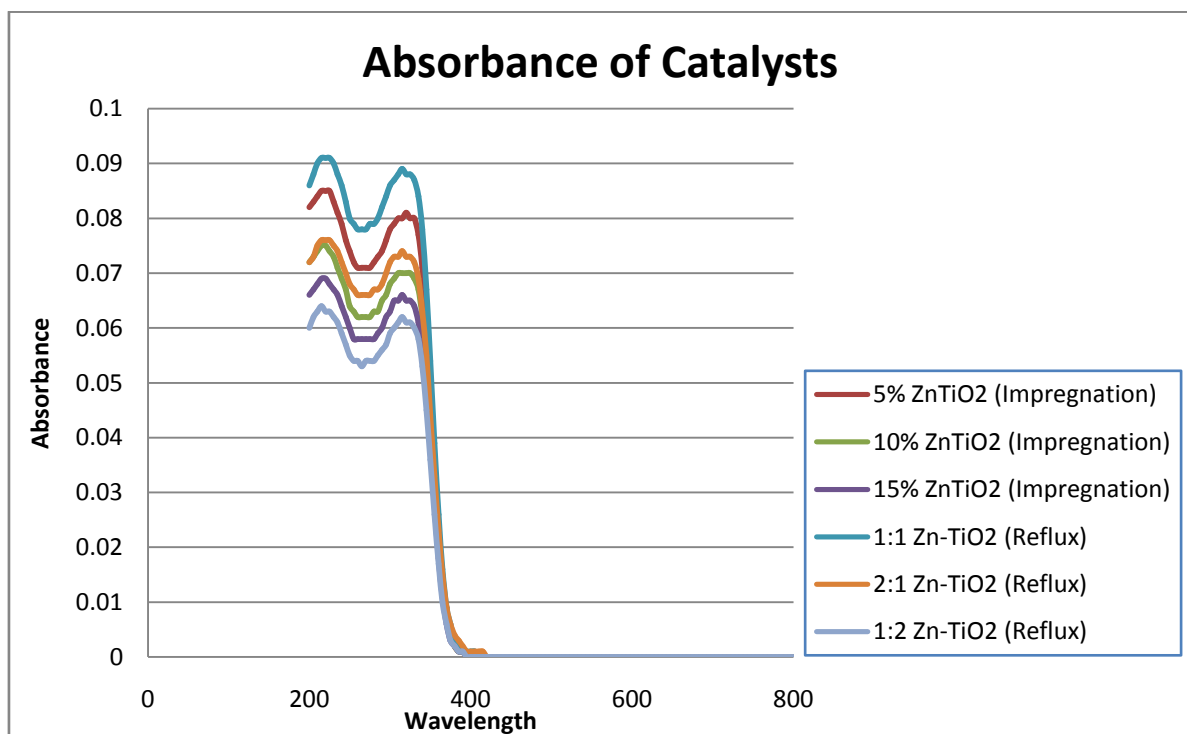


Figure 4.2 : Absorbance of the samples

Table 4.1: Band gap energy of zinc titanate

Sample	Band gap energy
5 wt% Zn-TiO ₂	3.24
10 wt% Zn-TiO ₂	3.25
15 wt% Zn-TiO ₂	3.26
1:1 Zn-TiO ₂	3.24
1:2 Zn-TiO ₂	3.22
2:1 Zn-TiO ₂	3.25

From the experiment, the 15wt% of Zn-TiO₂ by using impregnation method gives the highest value of band gap which is 3.26. The band gap will increase with the increasing amount of zinc in the sample. This is due the higher band gap energy of zinc as compared to titanium dioxide. Both methods show that the band gap of the sample increases with the amount of zinc. The improvement of band gap due to presence of zinc is good to reduce the recombination rate in DSSCs system, but if the amount of zinc is too high it will reduce the total efficiency as compared to bare TiO₂ electrode.

The solar energy conversion efficiency of DSSCs can be improved by the coating of ZnO as ZnO has bigger band gap compare to TiO₂ which is about 3.37 eV. ZnO also has the conduction band edge of (100 mV) more negative than that of TiO₂ as mention earlier by B.Posters et al. (2008). It show that the coating of ZnO on the TiO₂ contributes to provide an inherent energy barrier that suppressed charge recombination and improved voltage generated, resulting in an increase in conversion efficiency as well as fill factor compared to the single TiO₂ as reported by M.C. Kao et al.(2009).

4.1.2: Scanning Electron Microscopy (SEM)

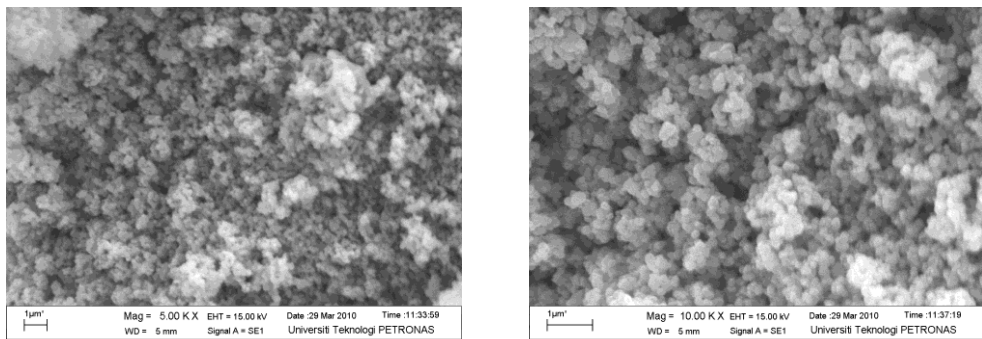


Figure 4.3: 1:1 mol ratio Zn-TiO₂

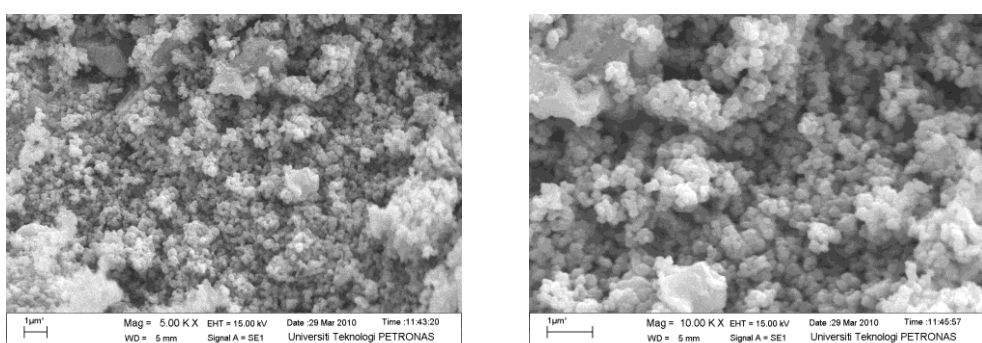


Figure 4.4: 1:2 mol ratio Zn-TiO₂

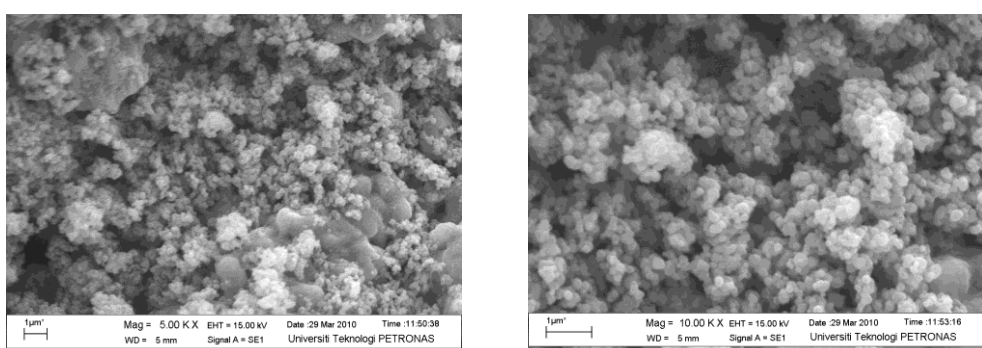


Figure 4.5: 2:1 mol ratio Zn-TiO₂

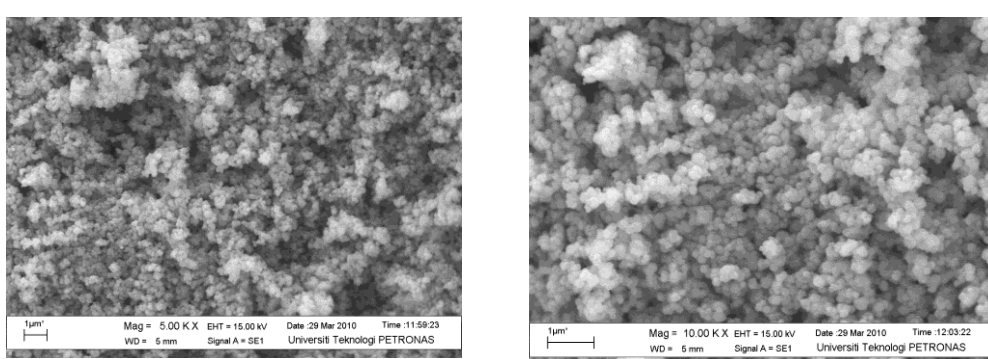


Figure 4.6: 5wt% Zn-TiO₂

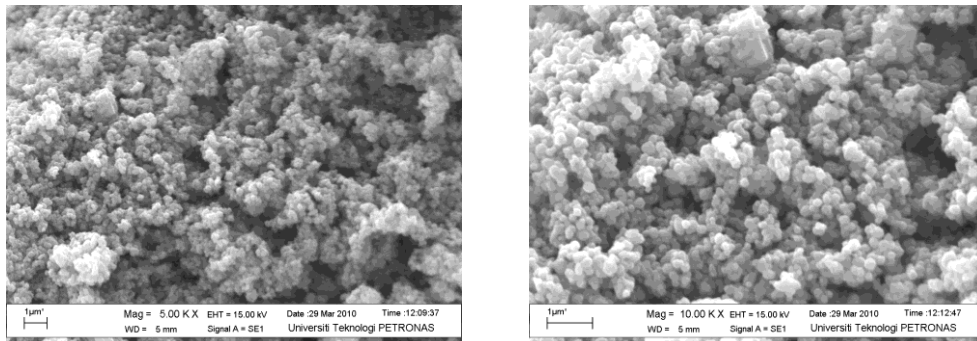


Figure 4.7: 10wt% Zn-TiO₂

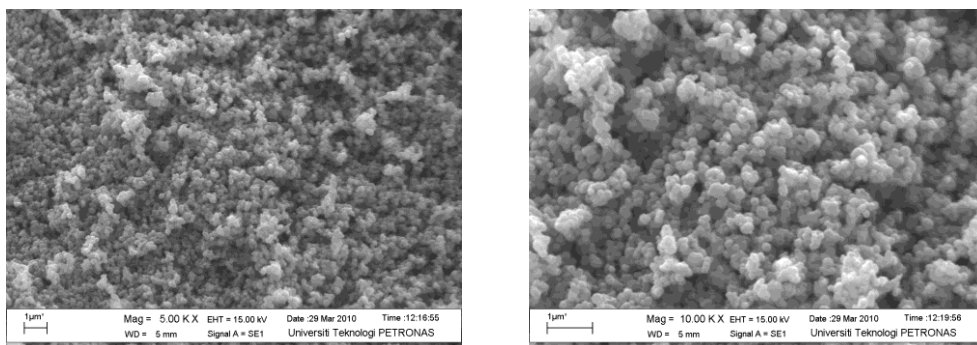


Figure 4.8: 15wt% Zn-TiO₂

Figures 4.3 to 4.8 are pictures taken by SEM on sample of the catalyst. In SEM analysis, the sample will undergo analysis where sample surface is analyzed using an electron. From the data, it shows how the component of the catalyst is distributed on the surface of catalyst. A good catalyst will have a well distributed component on the surface where reaction can take place. The existence zinc also provides more porous structure to the samples. Instead of having only TiO₂ compact structure molecule, zinc will provide more space for high mobility of ion in the DSSCs system. The deposited film from the suspensions of ZnO coated TiO₂ has also moderate porosity and high surface area to which dye molecule could be adsorbed as reported by S.S.Kim et. al. In a simple word, with zinc in the catalyst TiO₂ the efficiency of DSSCs will increases.

4.1.3: Fourier Transform Infrared (FTIR)

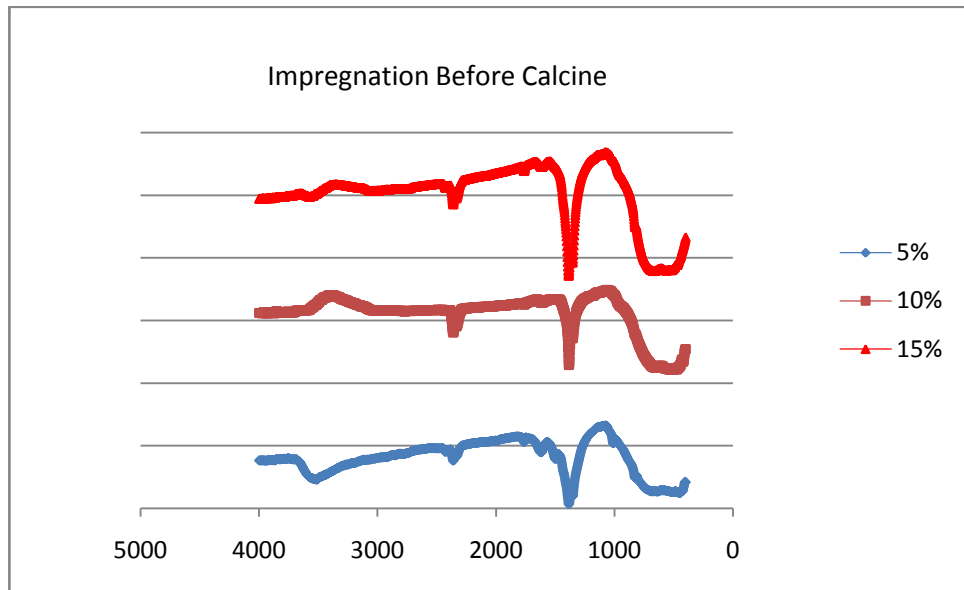


Figure 4.9: Impregnation before calcine

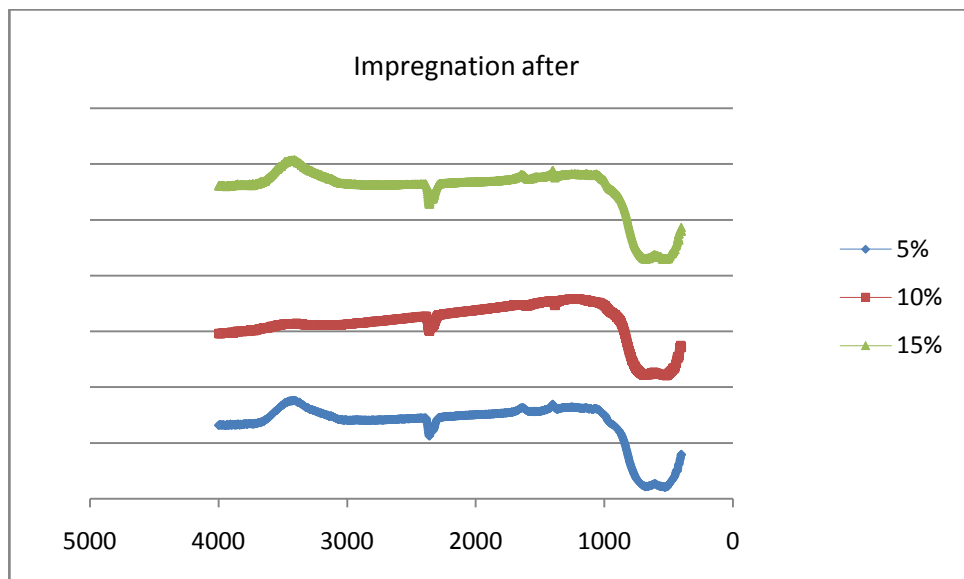


Figure 4.10: Impregnation after calcine

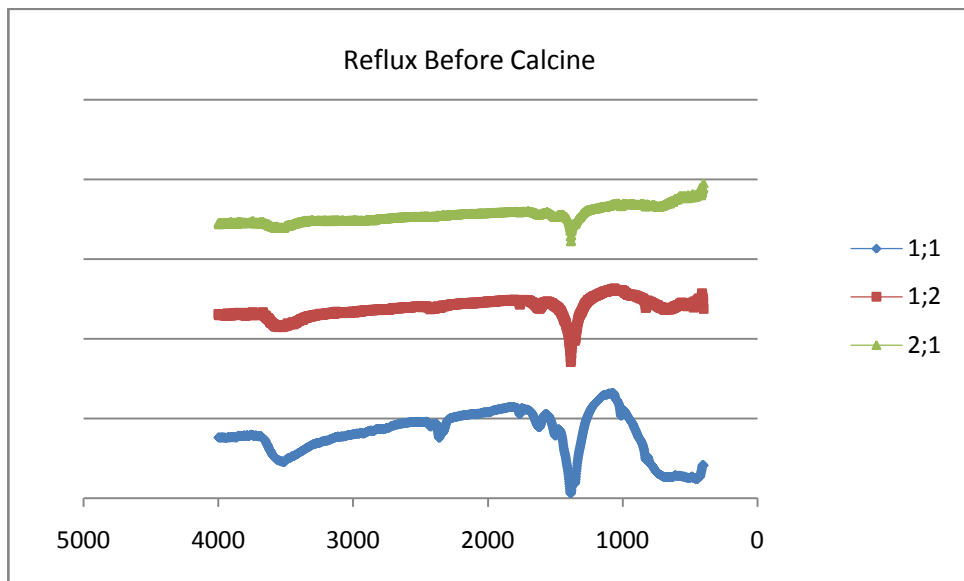


Figure 4.11: Reflux before calcine

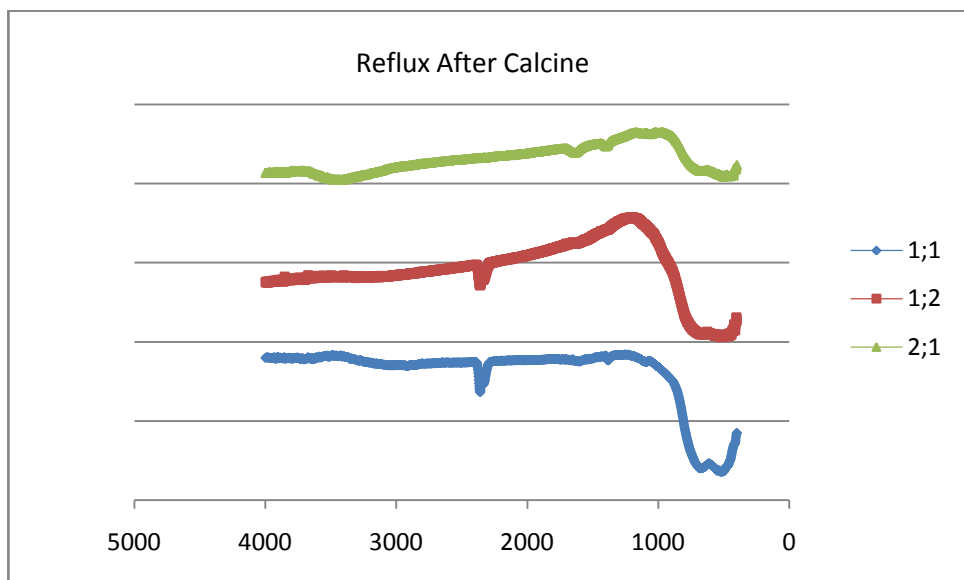


Figure 4.12: Reflux after calcine

FTIR results show the bonding in the sample. The absorption peak seen at approximately 1600cm^{-1} are known to be the O-H bending. As for the broad band seen around $400 - 900\text{cm}^{-1}$, that can be attributed to the Ti-O stretching vibrations. Furthermore, absorption peaks around 1384 cm^{-1} are due to the presence of NO_3^- . These peaks are visible in the spectra before calcinations, but are not present or unclear after calcinations. This goes to show that although nitrate groups were present during the preparation step of the catalysts, they were effectively removed after the calcination process.

4.1.4: X-ray Diffraction (XRD)

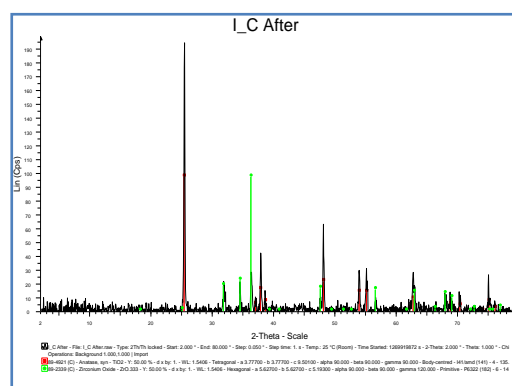
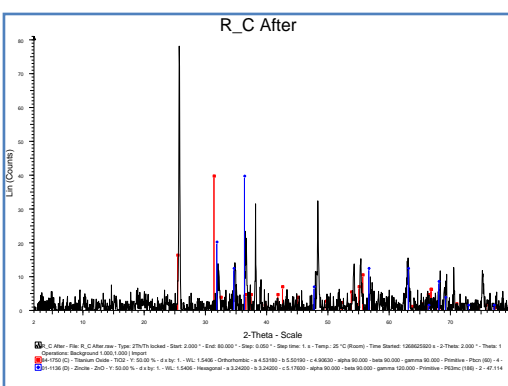
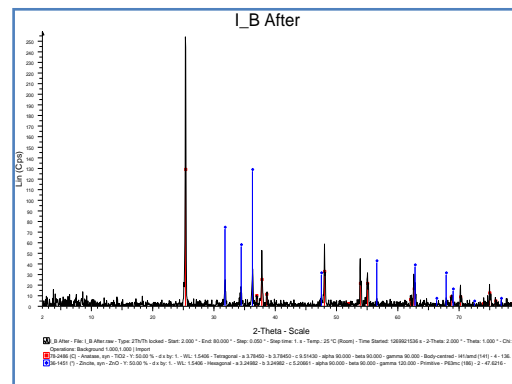
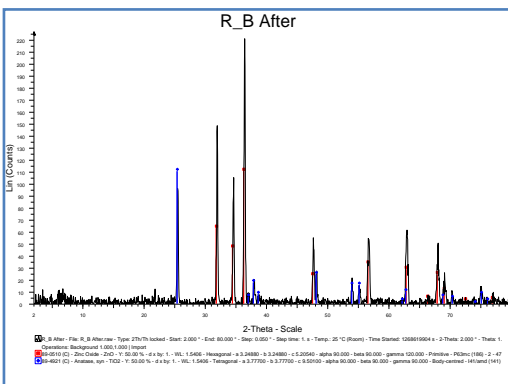
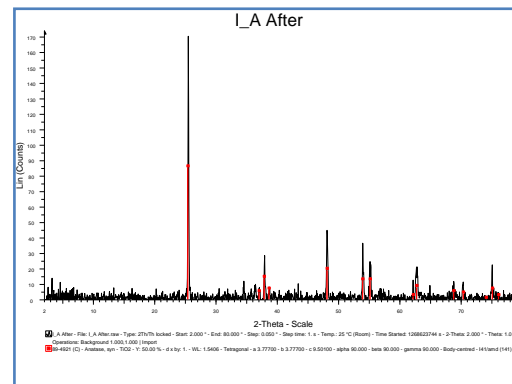
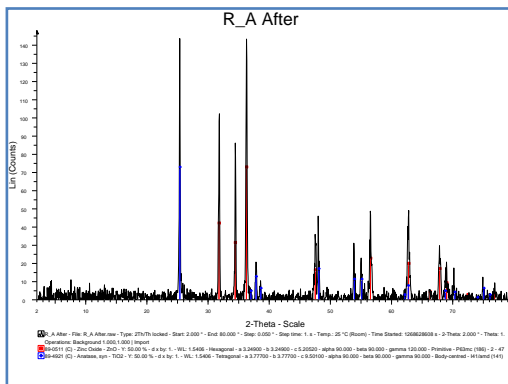


Figure 4.13: XRD result for reflux sample.

XRD result show that even with the presence of zinc in the sample, the anatase phase still can be maintained. The anatase phase structure is very important to prevent the recombination rate. The first peak from the left is the titanium dioxide peak and it's significant with the amount of titanium dioxide in the sample. The peak will be higher if the component is larger in the sample.

Figure 4.14: XRD result for impregnation sample.

From Figure 4.12, sample A (1:1 mol ratio Zn/TiO₂) the peak of anatase TiO₂ and ZnO clearly appears as both in the same mol ratio. The highest peak of TiO₂ is at $2\theta = 25^\circ$ and for ZnO is at $2\theta = 36^\circ$. For sample B (2:1 mol ratio Zn/TiO₂), the ZnO peak is the highest as the mol ratio of zinc to titanium increase. The figure also shows the reduction peak TiO₂ and increasing peak of ZnO. Sample C (1:2 mol ratio Zn/TiO₂) show the increasing peak of TiO₂ and reduction in ZnO peak. Figure 4.13 show the XRD result for 5%, 10%, and 15% amount of ZnO in TiO₂. The peak of TiO₂ is reducing as the amount of ZnO increases.

CHAPTER 5

CONCLUSION AND RECOMMENDATIONS

As conclusion, zinc titanate has been produced by using impregnation and reflux method. The catalysts undergo UV-vis analysis and the result shows that the highest band gap can be achieved by using impregnation method with 15% of ZnO in the total sample. From XRD, the anatase phase of TiO₂ still be maintain and no rutile phase detected. The anatase phase of the catalyst is very important to prevent the recombination rate of dye. FTIR analysis shows the nitrate group in the sample before calcine completely has been removed after calcine at temperature 500°C for 5 hours. SEM analysis shows the deposited film from the suspensions of ZnO coated TiO₂ has also moderate porosity and high surface area to which dye molecule could be adsorbed.

In this project, the highest efficiency that has been achieved is 3.26 by using impregnation method with 15 wt% zinc in the sample. Impregnation gives more time for the zinc nitrate and titanium oxide to mix well by continuously stirring the mixture for 5 hours. More time will provide finer tune catalyst. It's suggested that more sample to be produced so that the optimum ratio ZnO to TiO₂ can be determined. The calcinations temperature also can be varied to see the effect of calcinations temperature to the catalyst.

The limitation of equipment and chemical is one of the marvel problems in conducting final year project. Even it's the creativity of supervisor and student to deal with it, but the first objective of the project normally changed. The equipment seems to be there in lab but when the students want to use it, it already breakdown. So it's suggested that the equipment should be maintain or repair before the new coming semester as the student need it in completing the project. It will drag time and sometimes give difficulties to student in finishing their project.

REFERENCES

1. Janne Halme, 2002, *Dye-sensitized nanostructured and organic photovoltaic cells: technical review and preliminary tests*, Master's Thesis, Helsinki University, Finland.
2. Wataru Kubo, Ayumi Sakamoto, Takayuki Kitamura, Yuji Wada, Shozo Yanagida (2004), Dye-sensitized solar cells: improvement of spectral response by tandem structure, *Journal of Photochemistry and Photobiology A: Chemistry* 164, 33–39.
3. Tetsuo Soga (2006). Nanostructured Materials for Solar Energy Conversion (1st Ed.) Elsevier, UK.
4. Tae Woo Kim, Su Gil Hur, Seong-Ju Hwang, Jin-Ho Choy (2005), Layered titanate-zinc oxide nanohybrids with mesoporosity, *Chem Commun.* 2, 220-2.
5. Y.S. Chang, Y.H. Chang, I.G. Chen, G.J. Chen, Y.L. Chai (2002). Synthesis and Characterization of Zinc-Titanate Nano-crystal Powders by Sol-Gel Technique, *Journal of Crystal Growth*, 243, p.319-326.
6. N. Labus, N. Obradović, T. Srećković, V. Mitić, M.M. Ristić (2005). Influence of mechanical activation on synthesis of zinc metatitanate, *Science of Sintering*, 37, 115-122.
7. O. Yamaguchi, M. Morimi, H. Kawabata, K. Shimizu (1987), Formation and transformation of ZnTiO₃, *J. Am. Ceram. Soc.* 70, 97-98.
8. C.J Brinker, G.W. Scherer (1990), *Sol Gel Science*, Academic Press, New York.
9. F.H Dulin and D.E. Rase, Phase equilibria in the system ZnO-TiO₂ (1960). *J. Am. Ceramic Soc.* 43, 125-131.
10. J. Yang and J.H. Swisher (1996), The Phase Stability of Zn₂Ti₃O₈, *Materials Characterization* 37, 153-159.
11. Y.L. Chai, Y.S. Chang, G.J. Chen, Y.J. Hsiao (2008), The effects of heat treatment on the structure evolution and crystallinity of ZnTiO₃ nanocrystals prepared by Pechini process, *Materials Research Bulletin* 43, 1066-1073.
12. J.H Hyung, M. S. Akhtar, D.J. Kim, S.K. Lee (2009), ZnO nanowire covered TiO₂ thin film electrodes for improving the photovoltaic properties of Dye-sensitized Solar Cells, *Journal of the Korean Physical Society*, Vol. 55, pp. 89-93.

13. Sang Pang, Tengfeng Xie, Yu Zhang, Xiau Wei, Min Yang, Dejun Wang, (2007), Research on the effect of different sizes of ZnO nanorods on the efficiency of TiO₂ based Dye-Sensitized Solar Cells, *J. Phys. Chem. C*, 111, 18417-18422.
14. Ki Eun Kim, Song-Rim Jang, Jeunghee Park, R. Vittal, Kang-Jin Kim (2007), Enhancement in the performance of dye-sensitized solar cells containing ZnO-covered TiO₂ electrodes prepared by thermal chemical vapor deposition, *Solar Energy Materials and Solar Cells*, 91, 366-370.
15. Skoog, et al. *Principles of Instrumental Analysis*. 6th ed. Thomson Brooks/Cole. 2007, 169-173.
16. Hua Yu, Shanqing Zhang, Huijun Zhao, Geoffrey Will, Porun Liu (2008), An effective and low-cost TiO₂ compact layer for performance improvement of dye-sensitized solar cells, *Electrochimica Acta* 54, 1319-1324.
17. Yanan Fu, Zhengguo Jin, Yong Ni, Haiyan Du, Tao Wang (2009), Microstructure, optical and optoelectrical properties of mesoporous nc-TiO₂ films by hydrolysis-limited sol-gel process with different inhibitors, *Thin Solid Films*, 517, 5634-5640.
18. Seok-Soon Kim, Jun-Ho Yum, Yung-Eun Sung, 2005, Flexible dye-sensitized solar cells using ZnO coated TiO₂ nanoparticles, *Journal of Photochemistry and Photobiology A: Chemistry* 171, 269–273.
19. Mingdeng Wei et al. (2006), Highly efficient dye-sensitized solar cells composed of mesoporous titanium dioxide *J. Mater. Chem.*, 16, 1287–1293.
20. S. Brunauer, P. H. Emmett and E. Teller (1938), *J. Am. Chem. Soc.*, 60, 309.
21. M.C. Kao, H.Z. Chen, S.L. Young (2009), Effect of ZnO coating on the performance of TiO₂ nanostructured thin films for dye sensitized solar cells, *Applied Physics A*, 97, 469-474.

APPENDICES

Appendix A: XRD (before and after calcine)

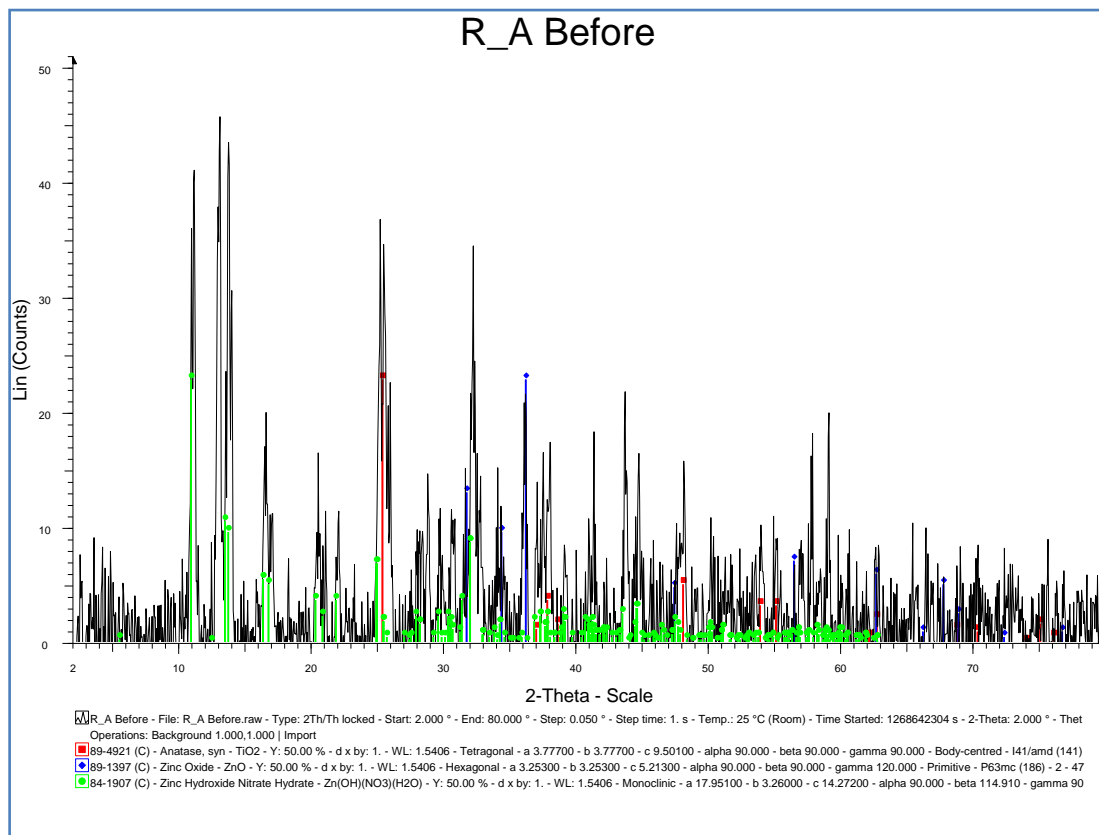


Figure 1: Reflux 1:1 before calcine

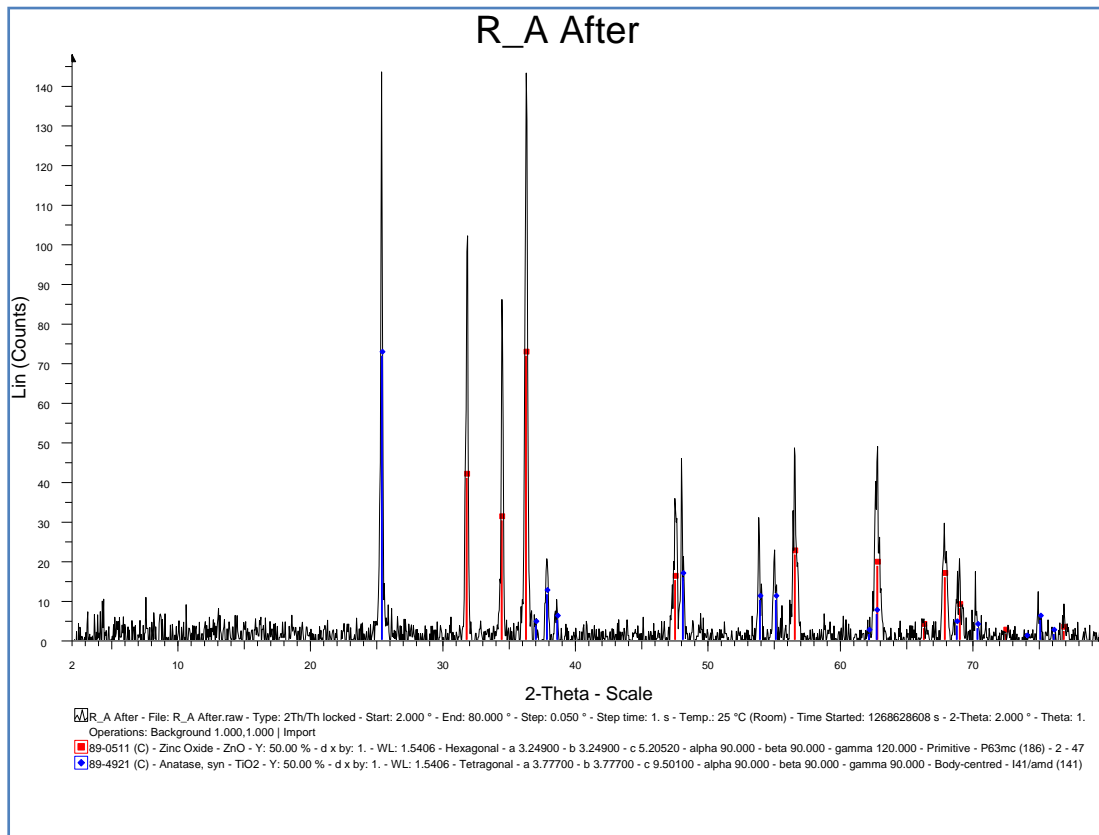


Figure 2: Reflux 1:1 after calcine

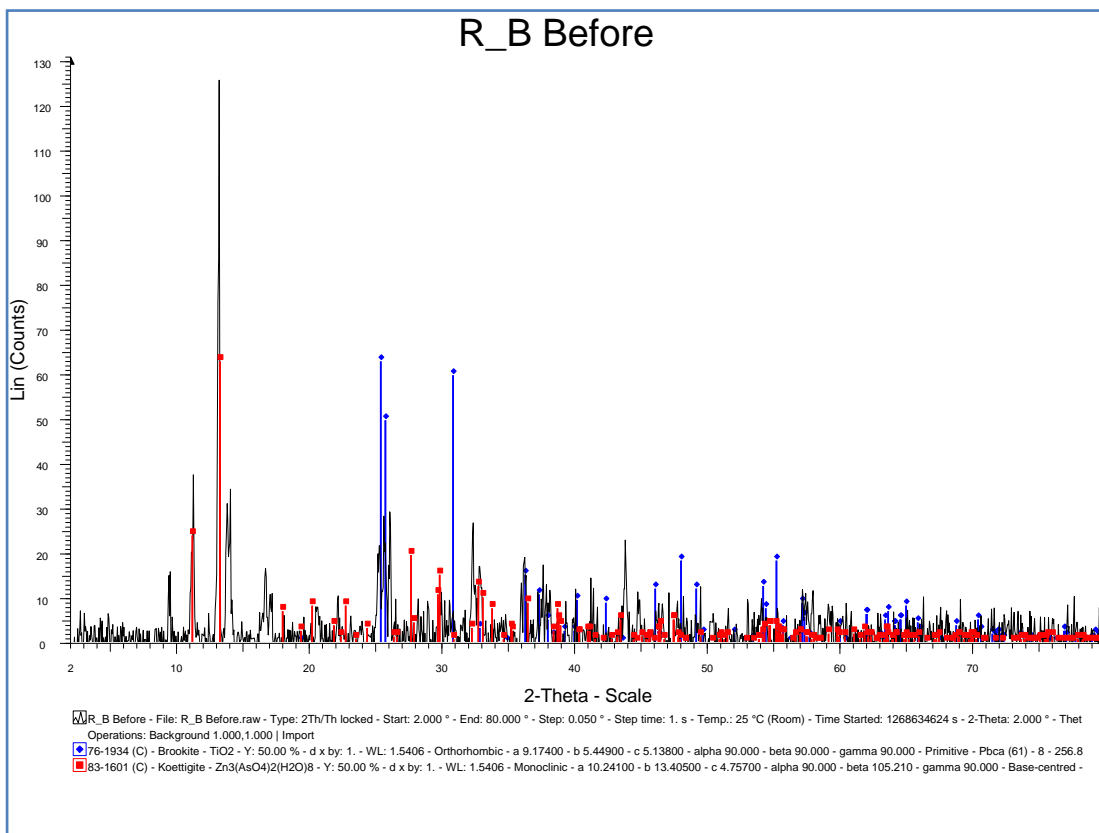


Figure 3: Reflux 1:2 before calcine

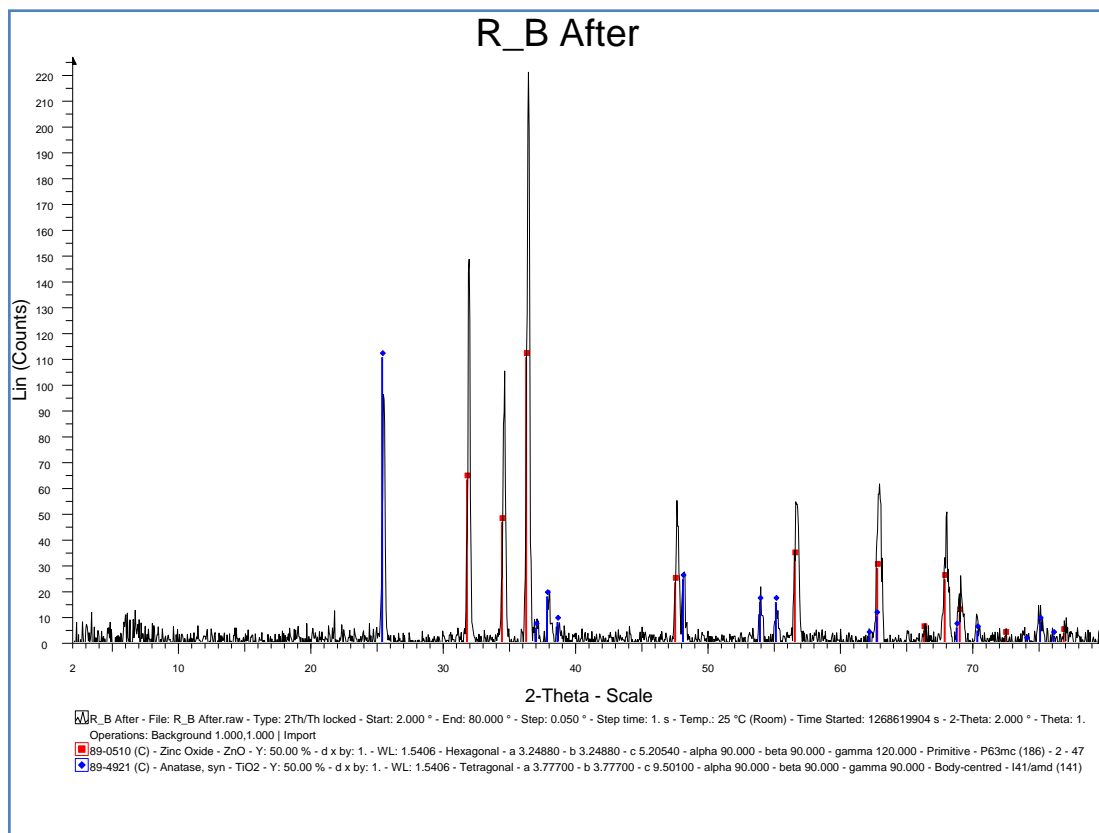


Figure 4: Reflux 1:2 after calcine

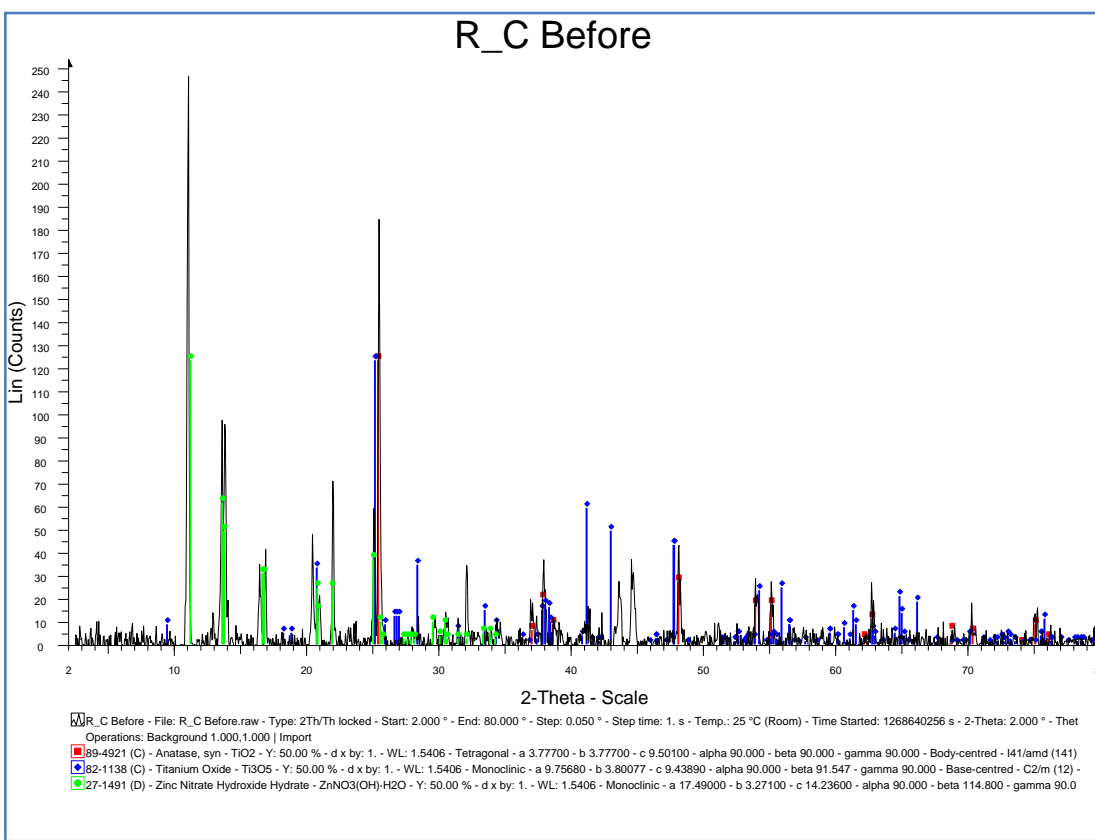


Figure 5: Reflux 2:1 before calcine

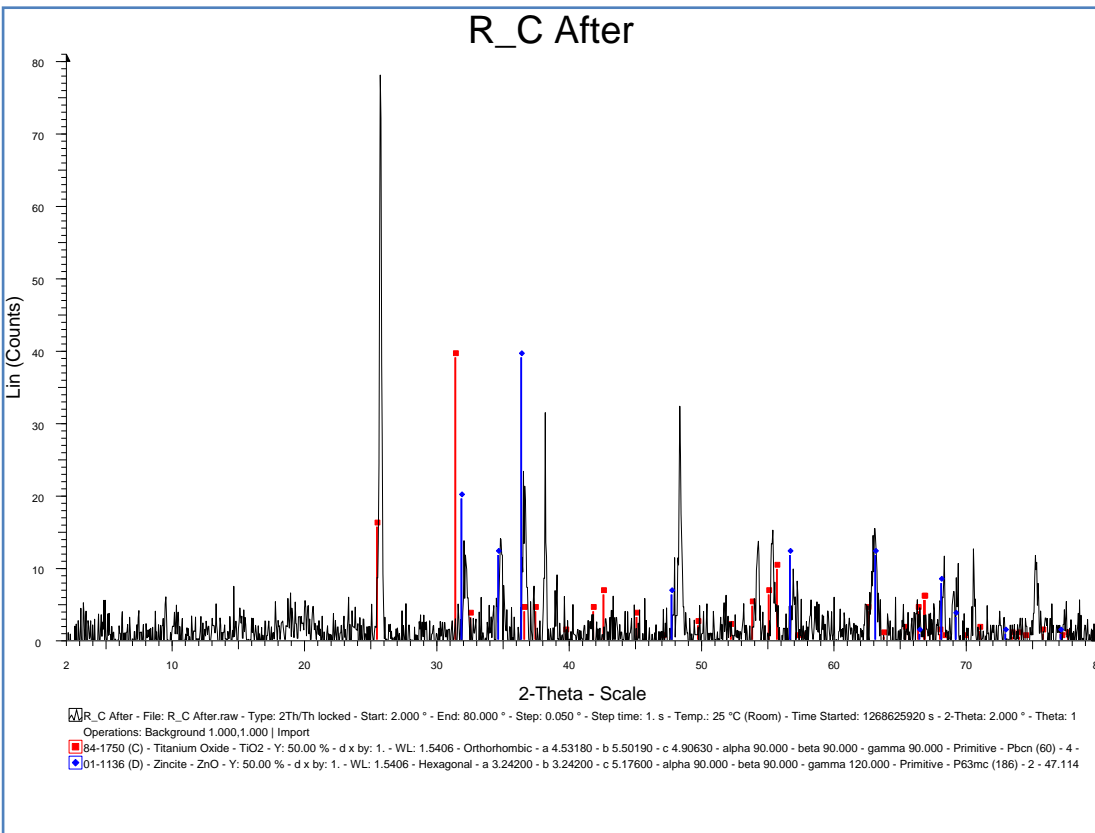


Figure 6: Reflux 2:1 after calcine

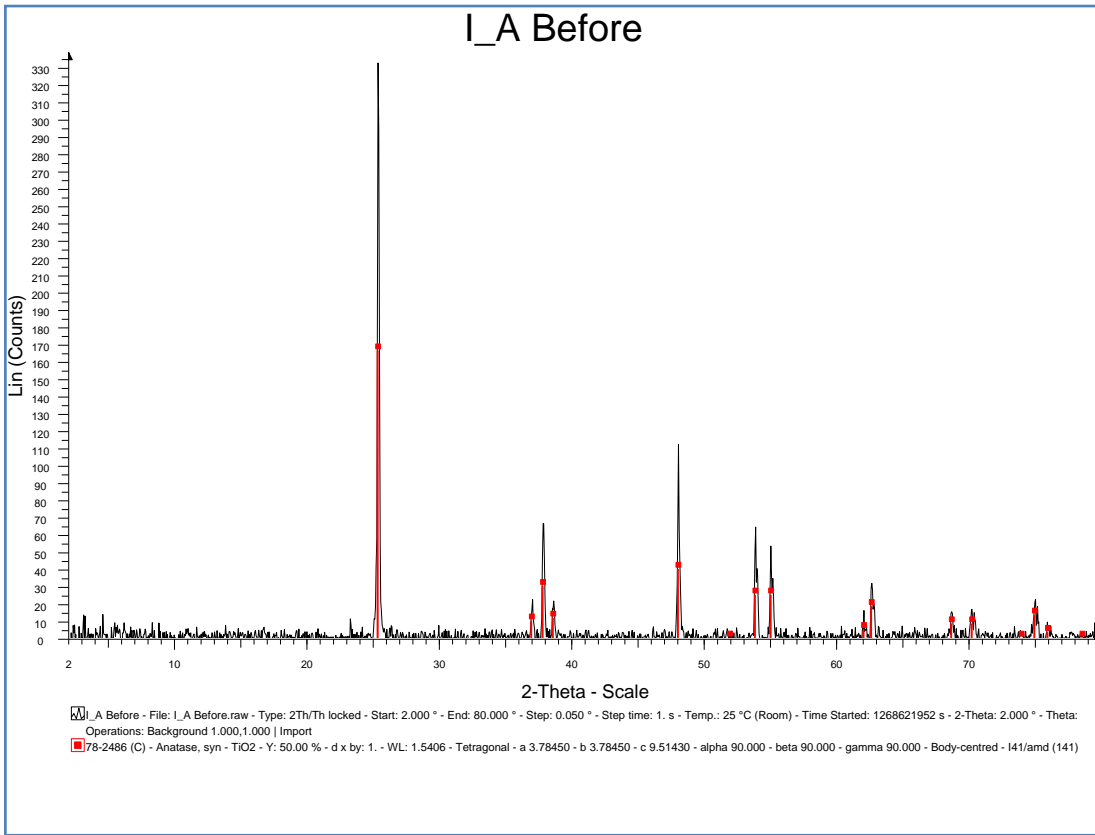


Figure 7: Impregnation 5% before calcine

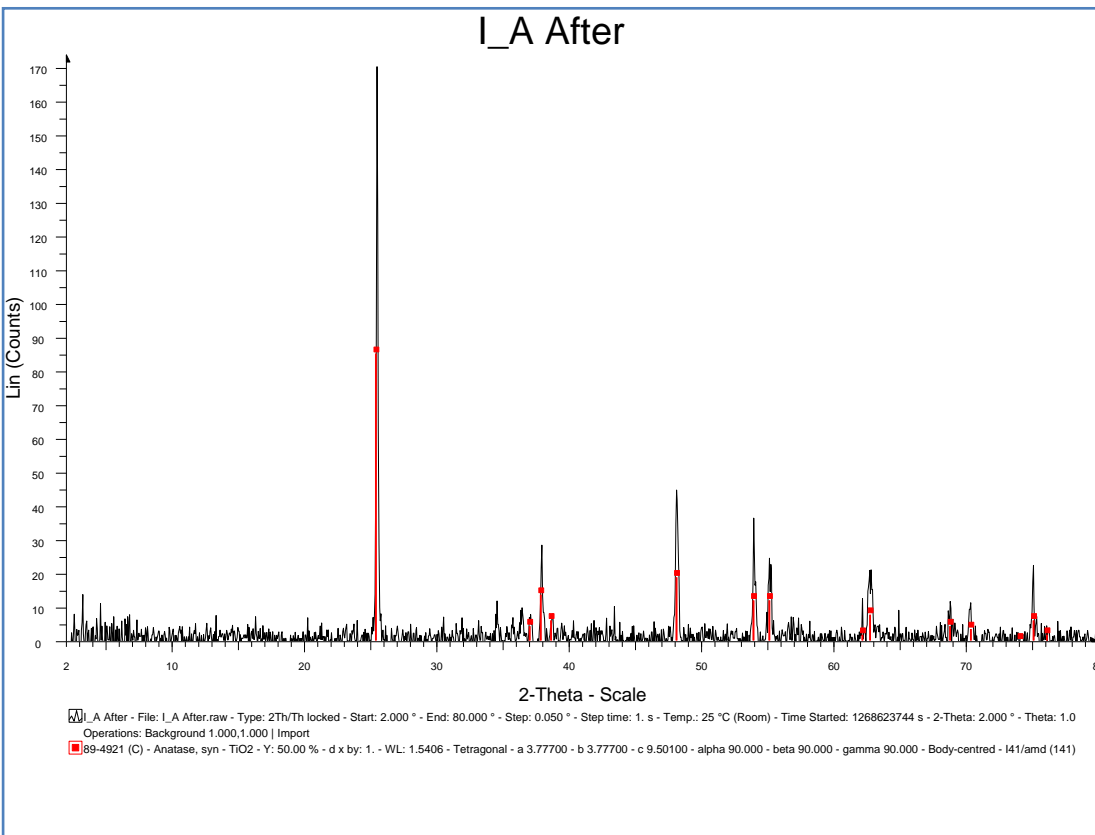


Figure 8: Impregnation 5% after calcine

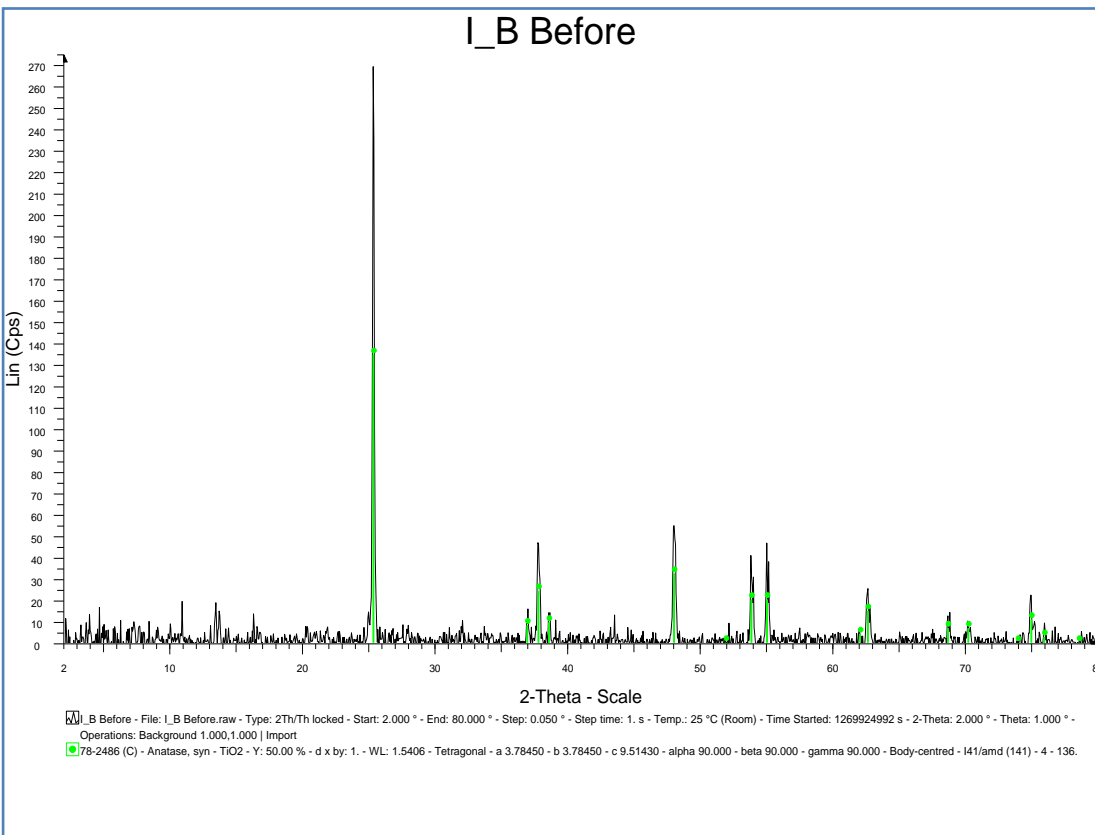


Figure 9: Impregnation 10% before calcine

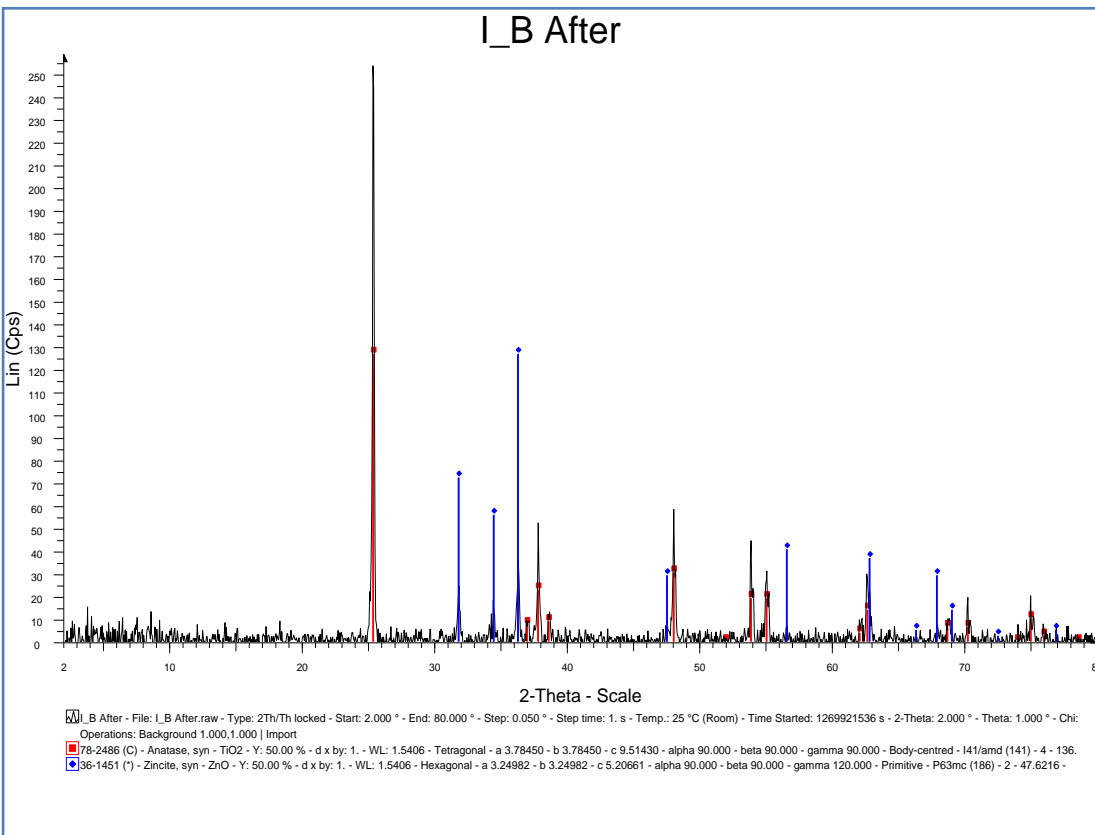


Figure 10: Impregnation 10% after calcine

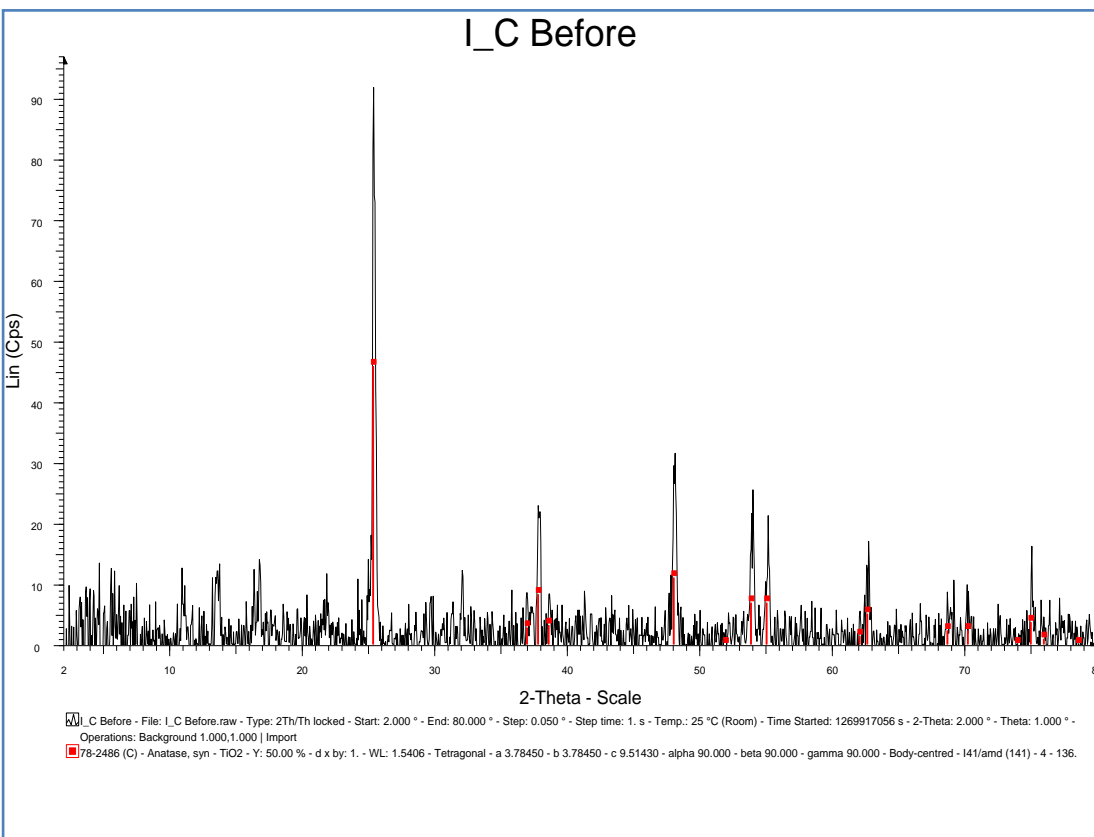


Figure 11: Impregnation 15% before calcine

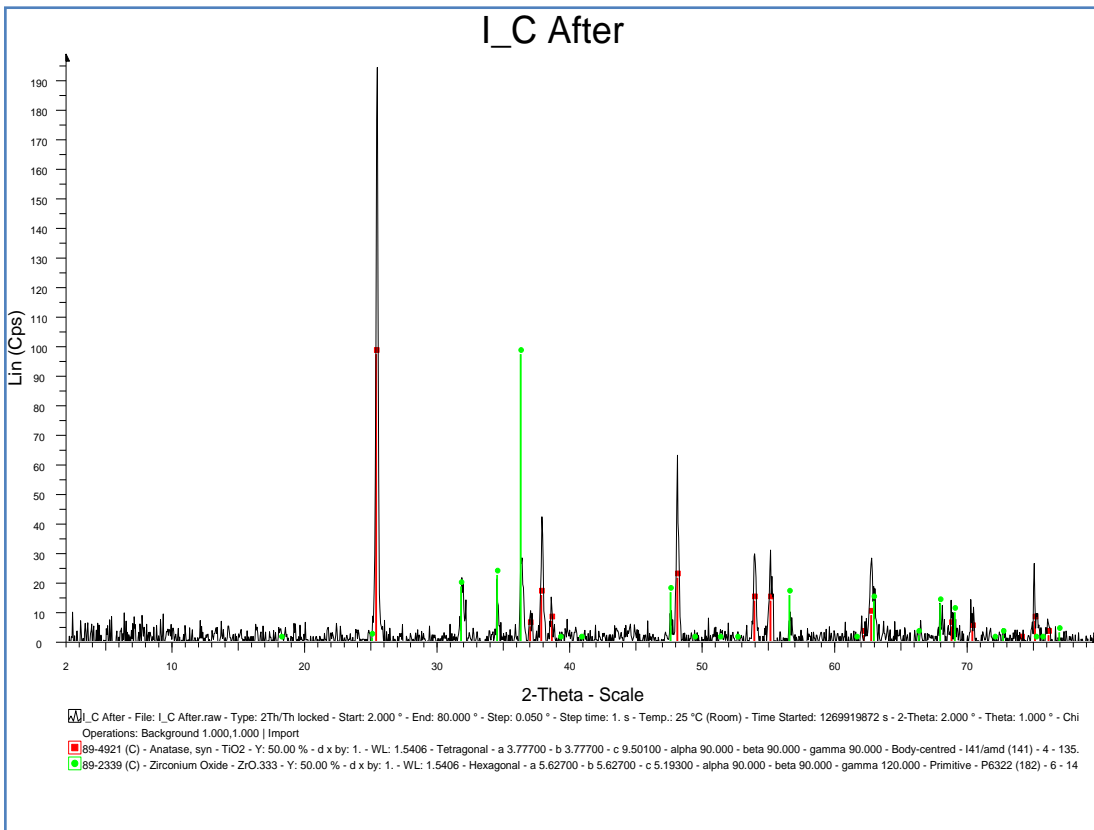


Figure 12: Impregnation 15% after calcine

Appendix B: FTIR (before and after calcine)

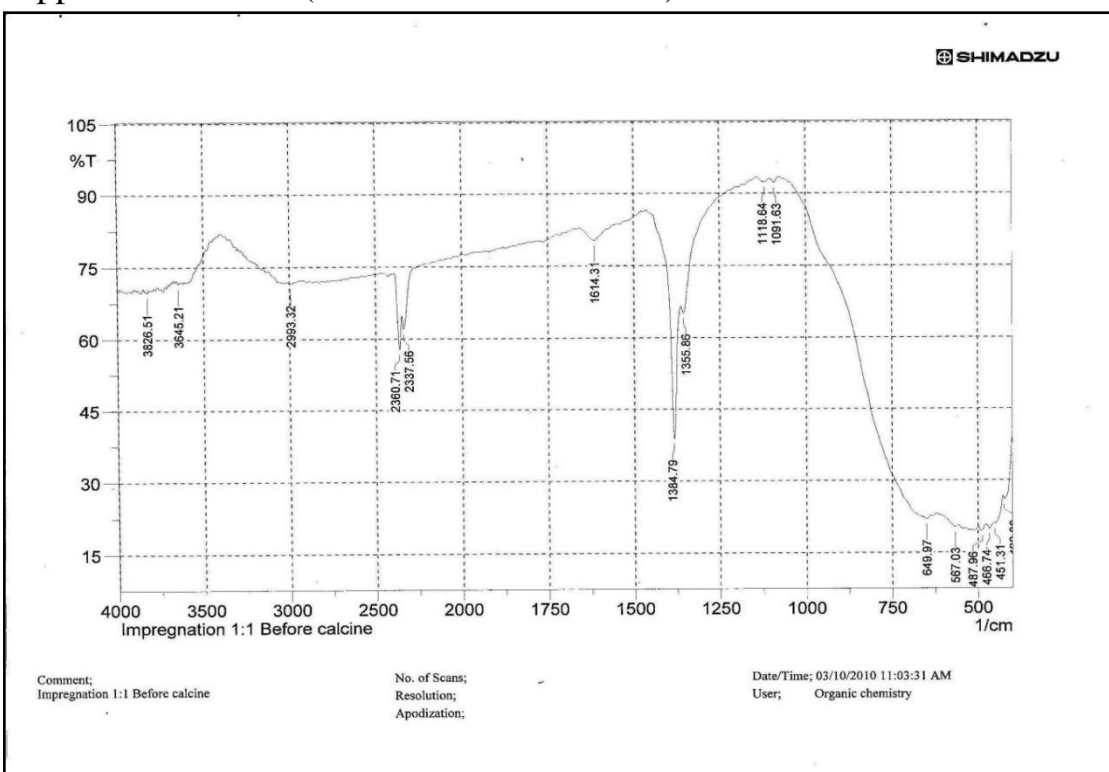


Figure 13: Impregnation 5% before calcine

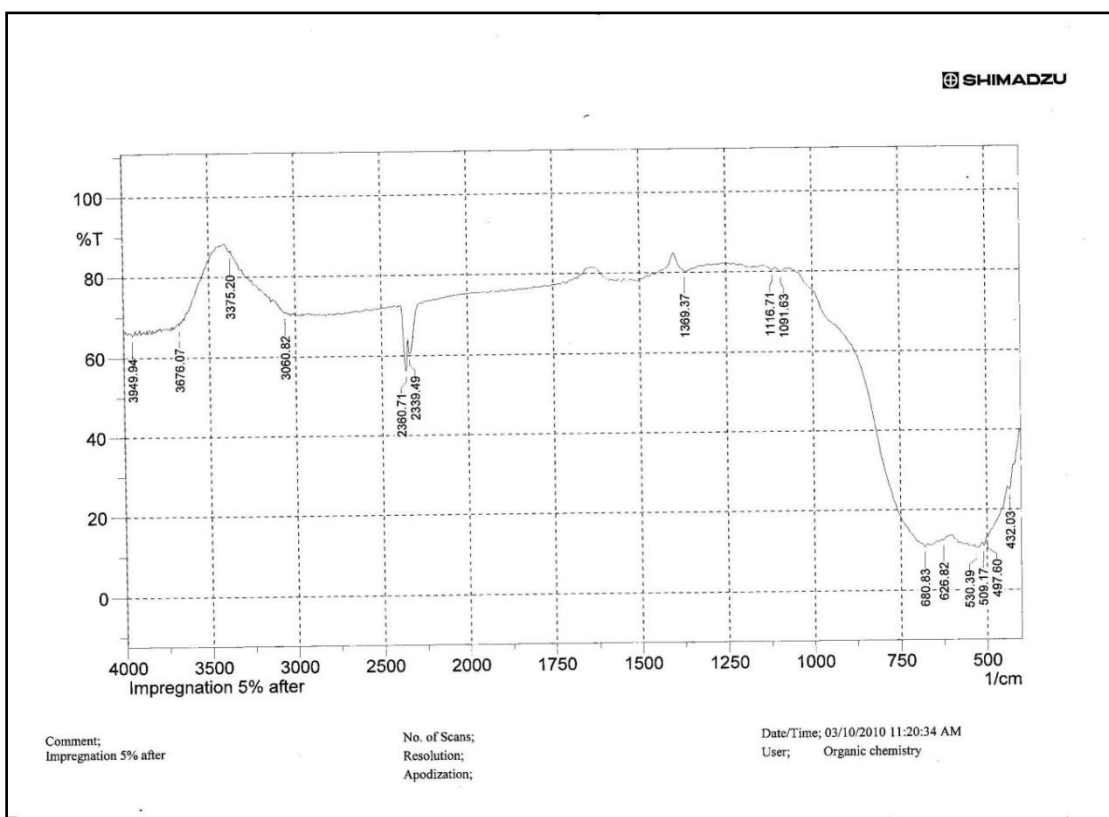


Figure 14: Impregnation 5% after calcine

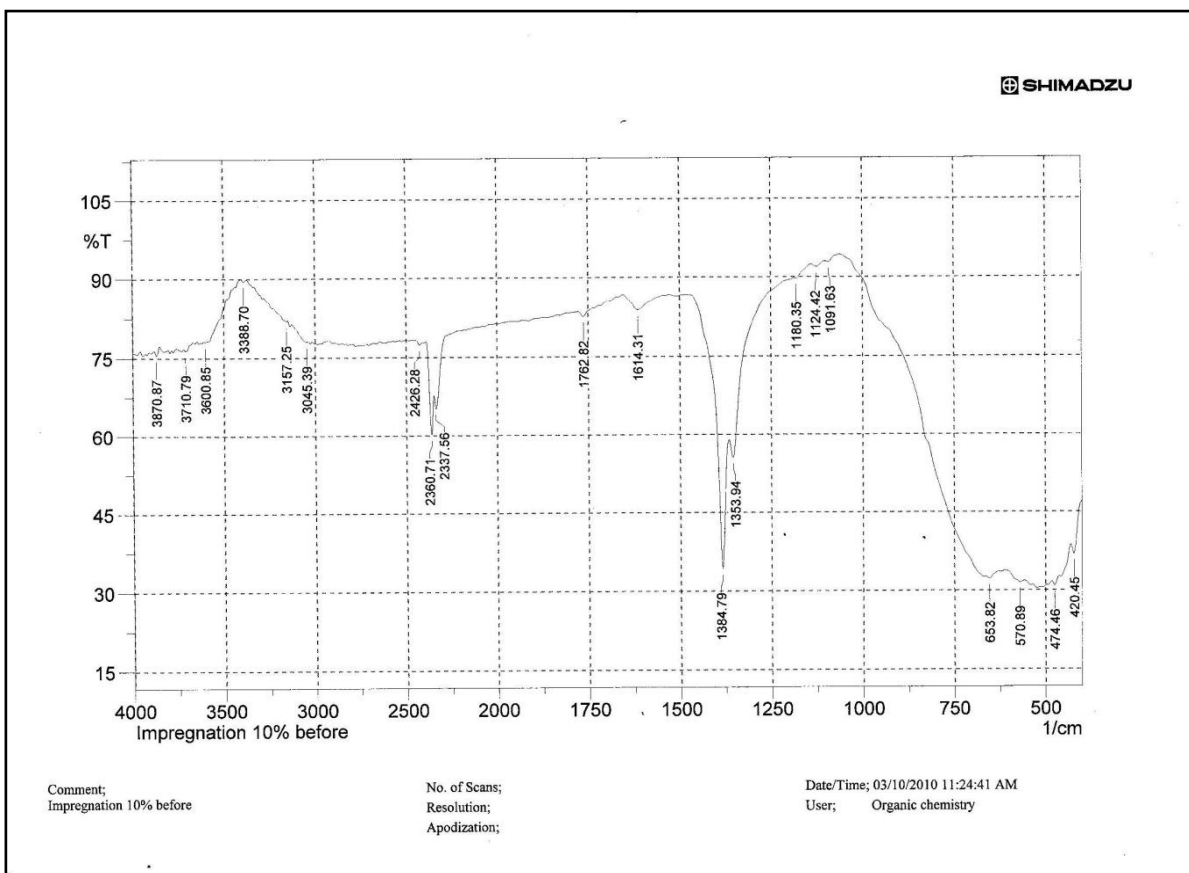


Figure 15: Impregnation 10% before calcine

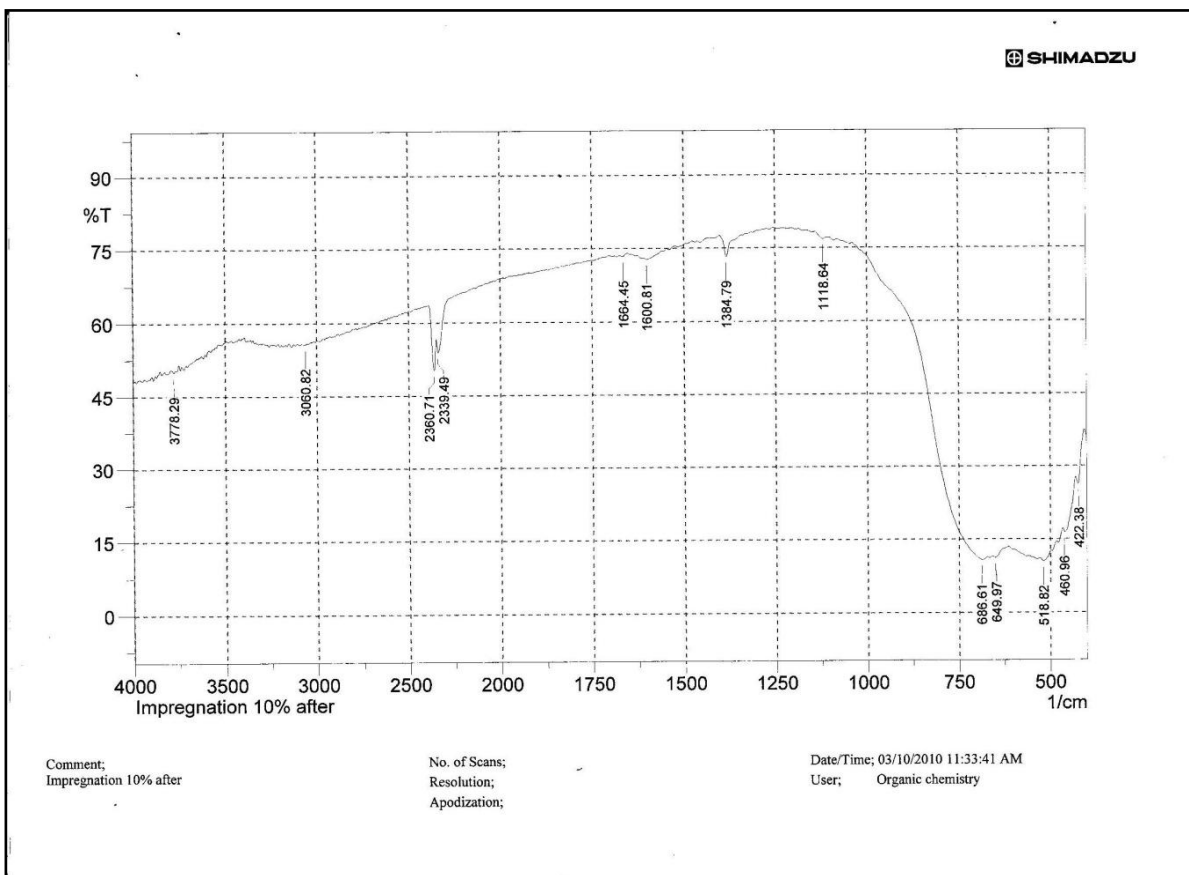


Figure 16: Impregnation 10% after calcine

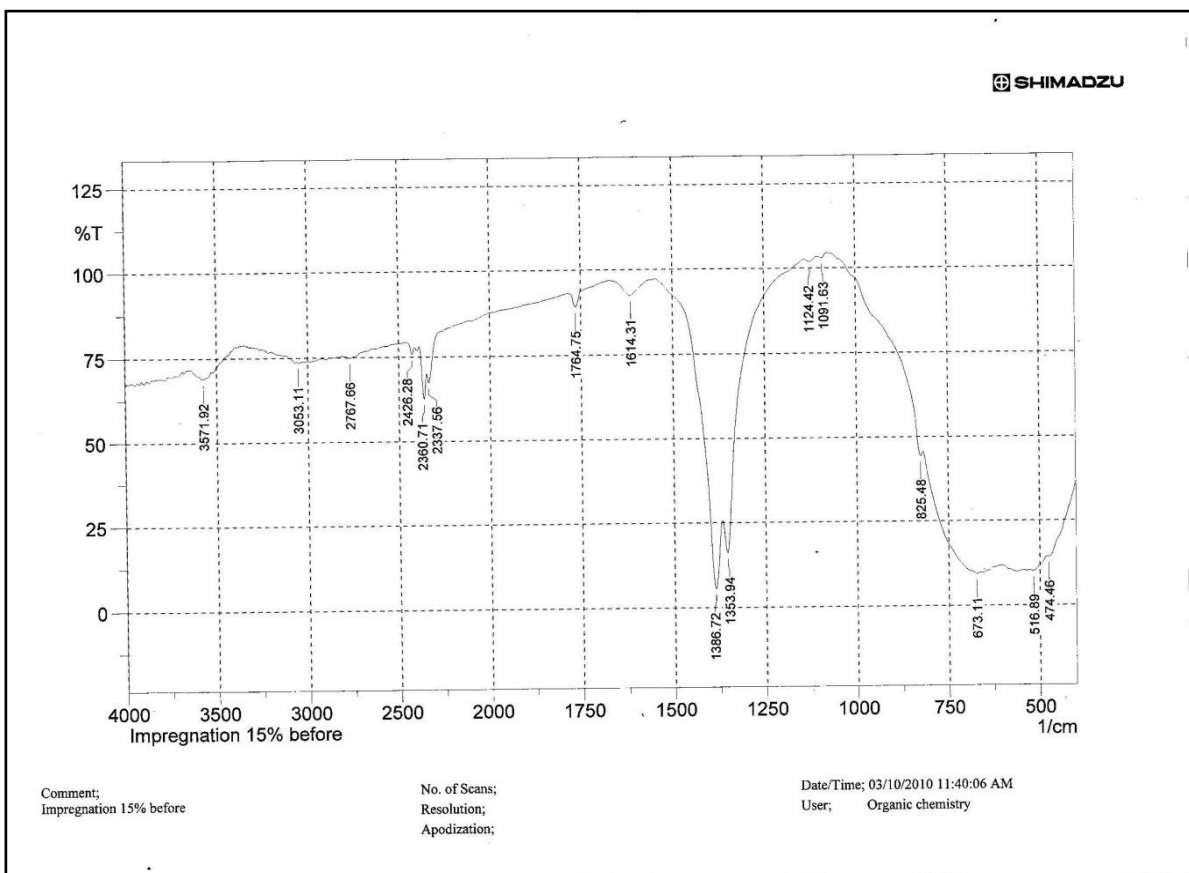


Figure 17: Impregnation 15% before calcine

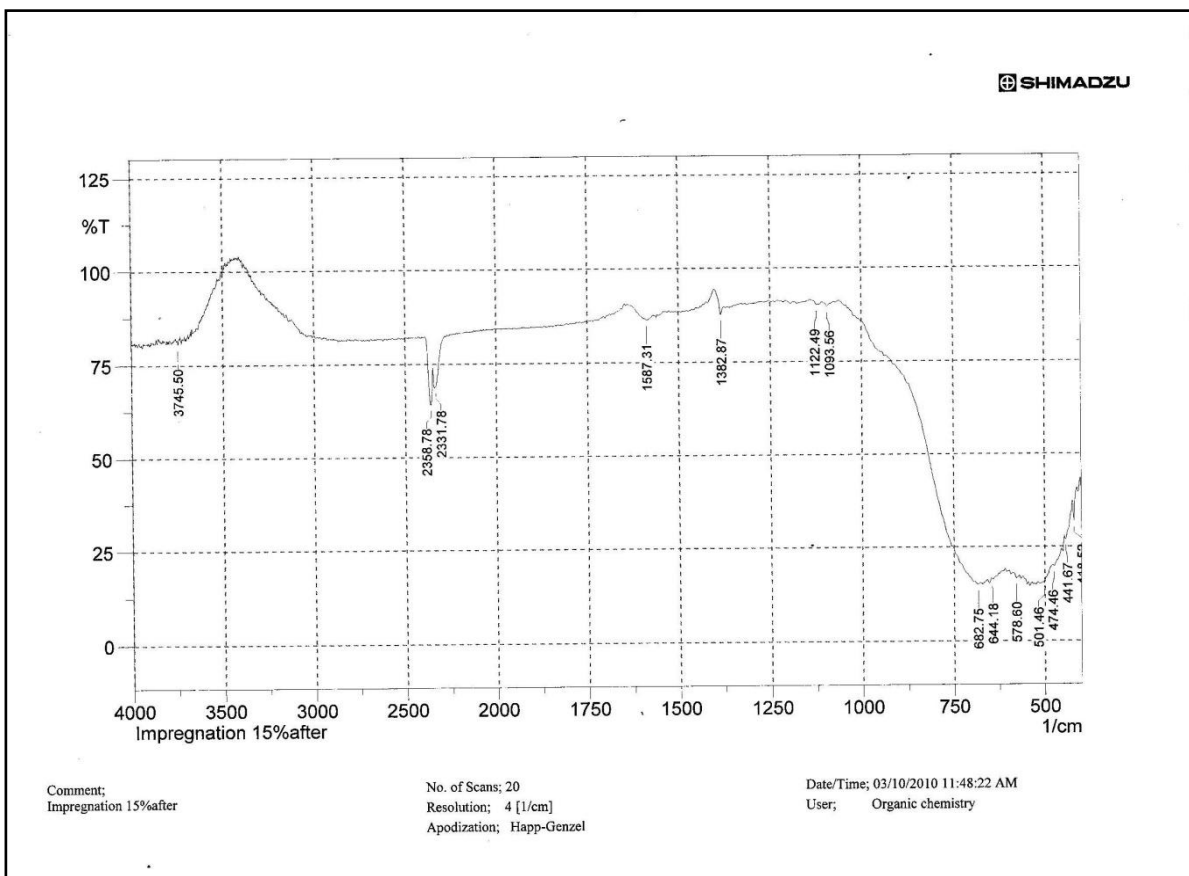


Figure 18: Impregnation 15% after calcine

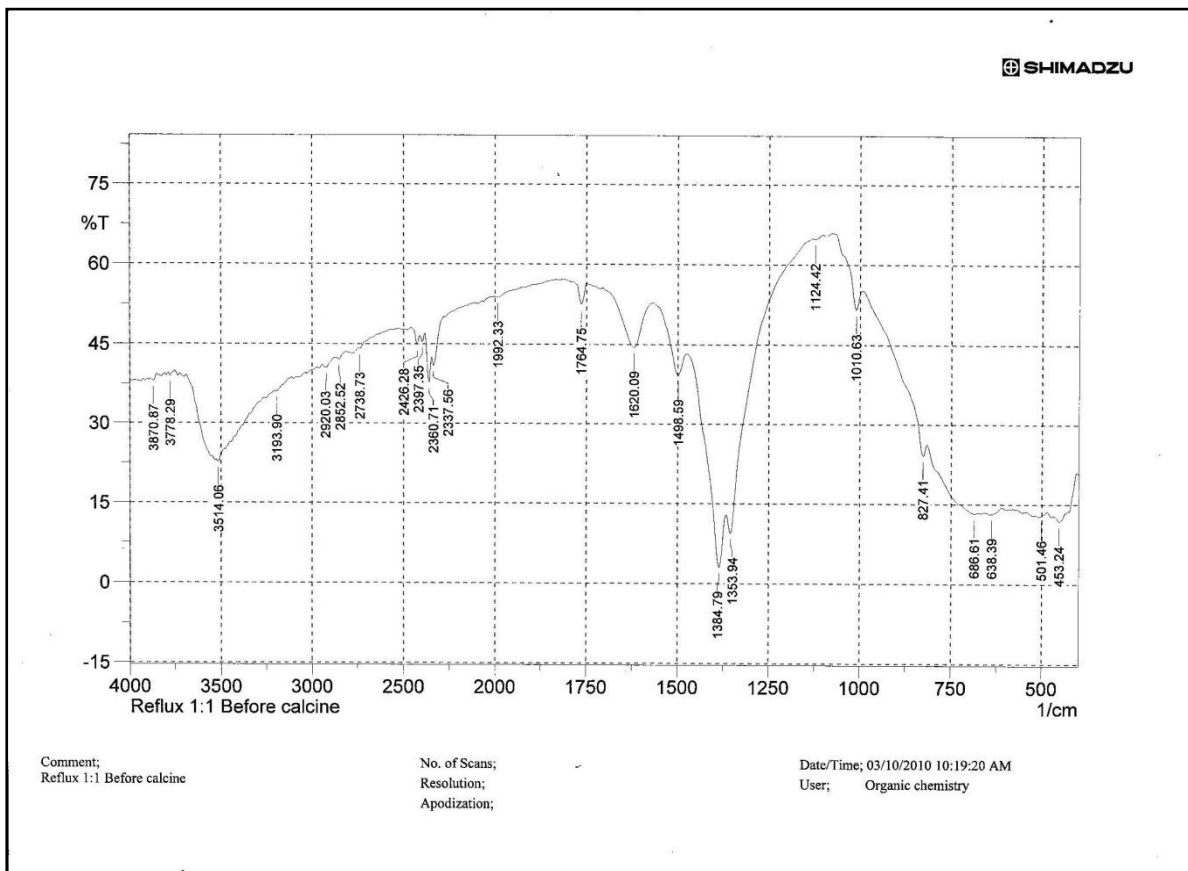


Figure 19: Reflux 1:1 before calcine

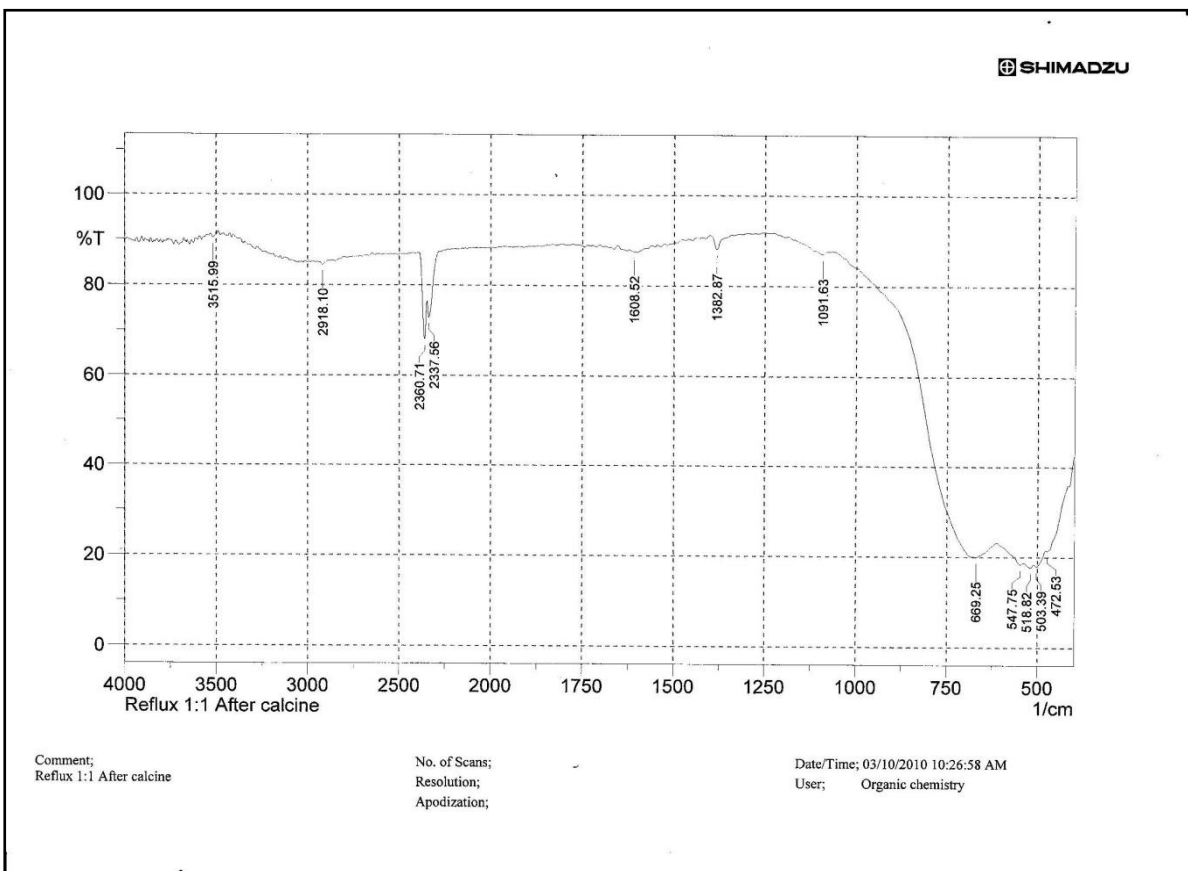


Figure 20: Reflux 1:1 after calcine

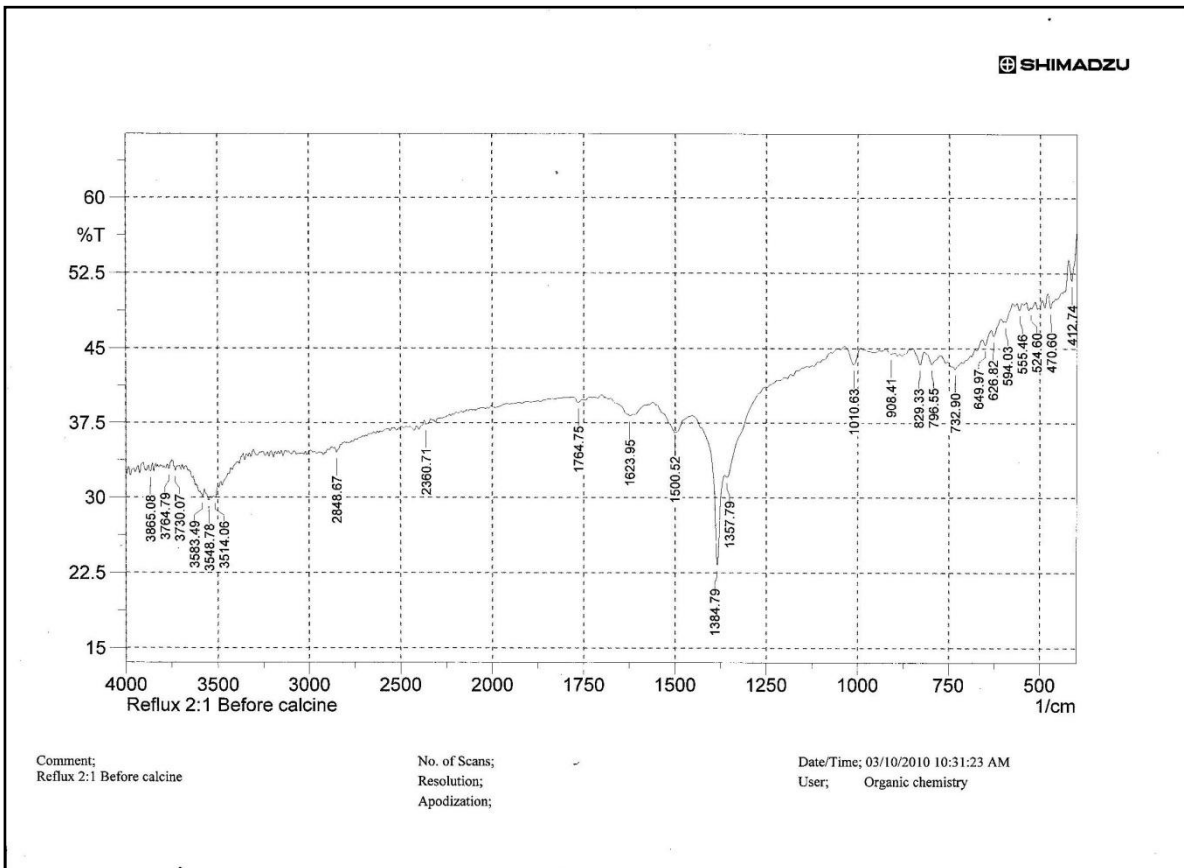


Figure 21: Reflux 1:2 before calcine

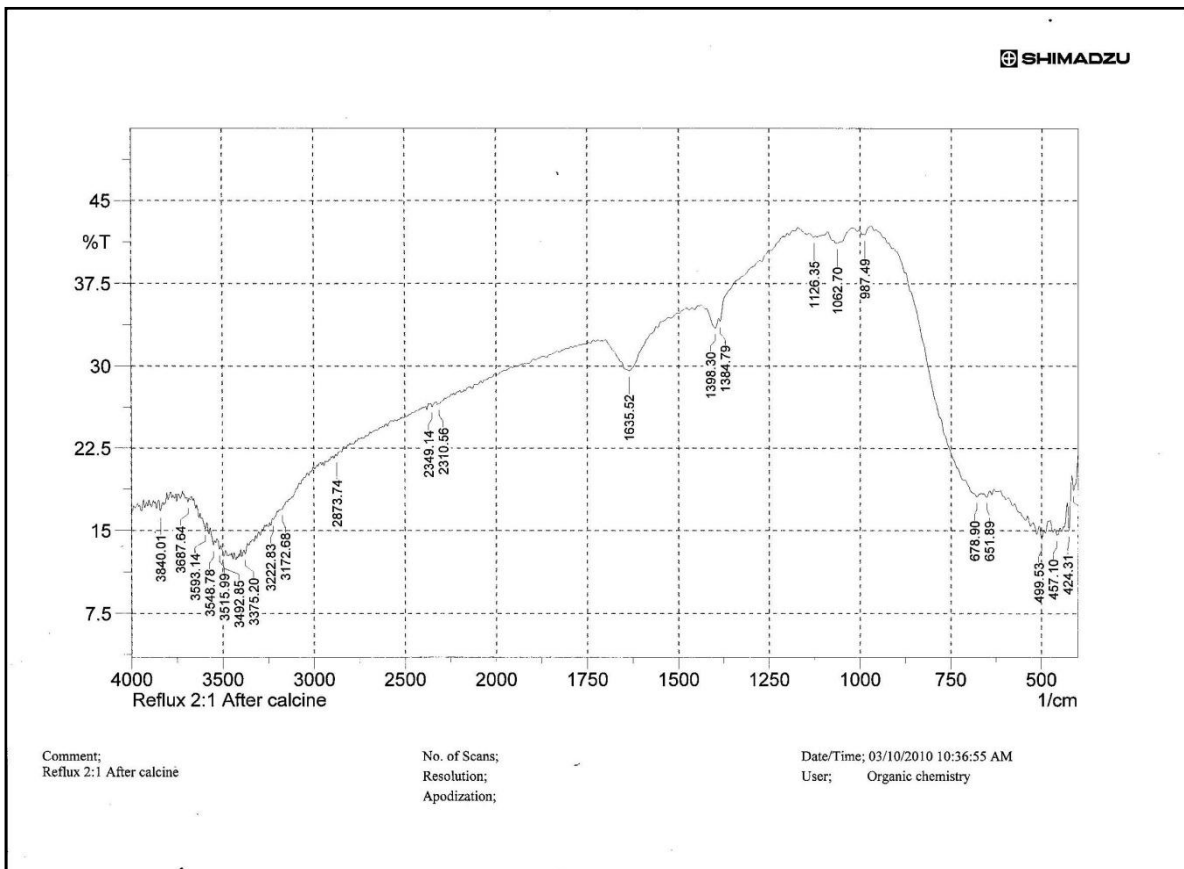


Figure 22: Reflux 1:2 after calcine

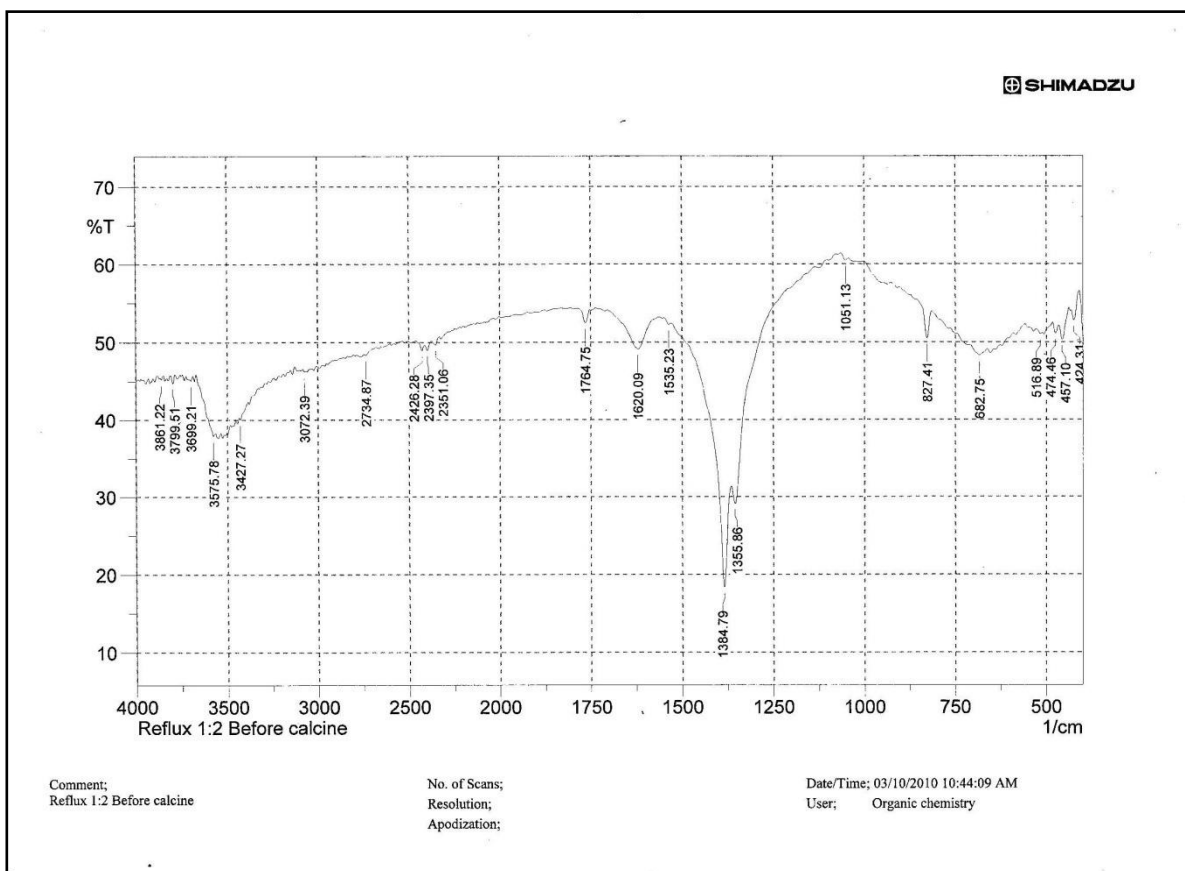


Figure 23: Reflux 2:1 before calcine

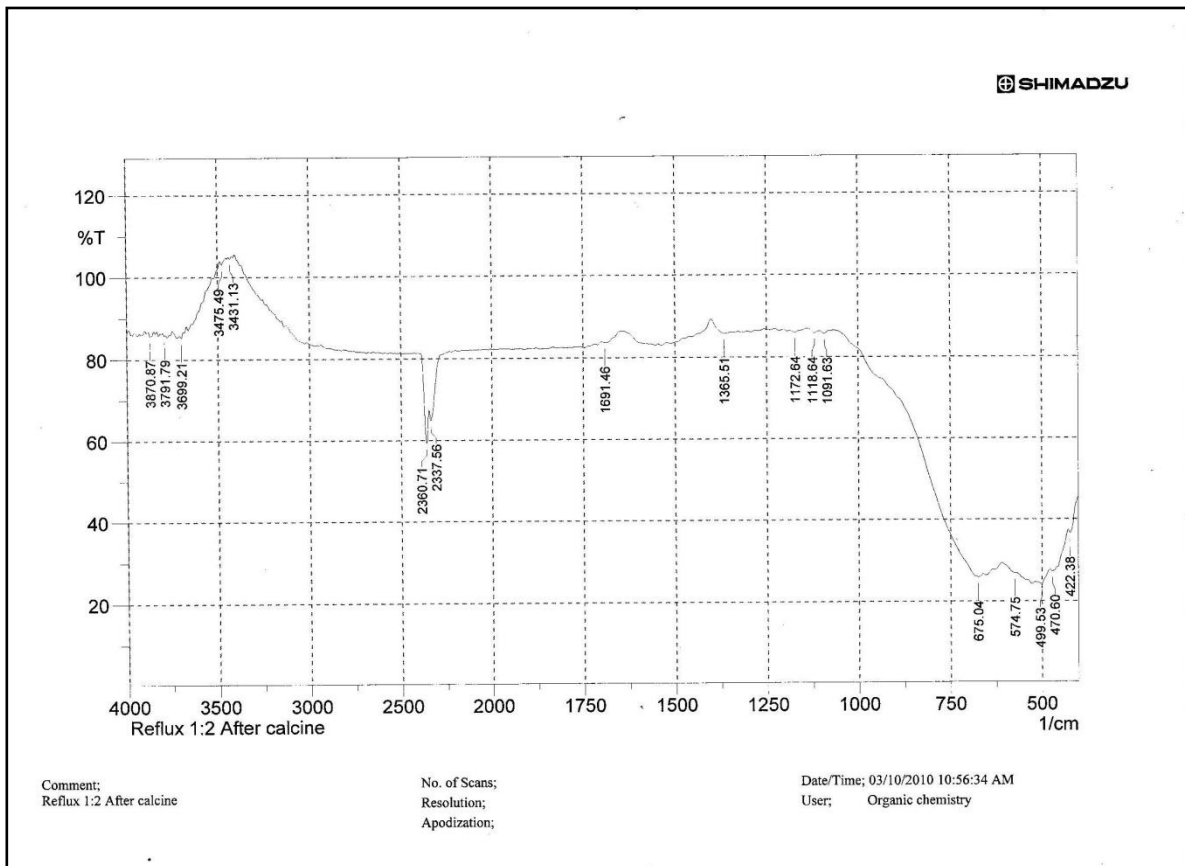


Figure 24: Reflux 2:1 after calcine

Appendix C: UV-vis (calculation)

Table 1: Impregnation 5%

5% ZnTiO2 (Impregnation)							
wavelength	% Reflectance	Reflectance	F(R)=(1-R)^2/(2R)	v=c/wavelength	E=hv	sqrt(F(R)*E)	Absorbance
800	90.038	0.90038	0.005511087	3.74741E+14	1.55	0.09	0
795	89.984	0.89984	0.005574339	3.77097E+14	1.56	0.09	0
790	89.922	0.89922	0.005647455	3.79484E+14	1.57	0.09	0
785	89.955	0.89955	0.005608472	3.81901E+14	1.58	0.09	0
780	89.909	0.89909	0.005662852	3.84349E+14	1.59	0.09	0
775	89.888	0.89888	0.005687775	3.86829E+14	1.60	0.10	0
770	89.859	0.89859	0.005722292	3.89341E+14	1.61	0.10	0
765	89.868	0.89868	0.005711567	3.91886E+14	1.62	0.10	0
760	89.9	0.899	0.005673526	3.94464E+14	1.63	0.10	0
755	89.888	0.89888	0.005687775	3.97076E+14	1.64	0.10	0
750	89.874	0.89874	0.005704424	3.99723E+14	1.65	0.10	0
745	89.868	0.89868	0.005711567	4.02406E+14	1.66	0.10	0
740	89.888	0.89888	0.005687775	4.05125E+14	1.68	0.10	0
735	89.882	0.89882	0.005694907	4.07881E+14	1.69	0.10	0
730	89.896	0.89896	0.005678274	4.10675E+14	1.70	0.10	0
725	89.879	0.89879	0.005698475	4.13507E+14	1.71	0.10	0
720	89.877	0.89877	0.005700854	4.16378E+14	1.72	0.10	0
715	89.865	0.89865	0.005715141	4.1929E+14	1.73	0.10	0
710	89.862	0.89862	0.005718716	4.22243E+14	1.75	0.10	0
705	89.87	0.8987	0.005709185	4.25238E+14	1.76	0.10	0
700	89.879	0.89879	0.005698475	4.28275E+14	1.77	0.10	0
695	89.893	0.89893	0.005681836	4.31356E+14	1.78	0.10	0
690	89.935	0.89935	0.00563208	4.34482E+14	1.80	0.10	0
685	89.964	0.89964	0.005597867	4.37653E+14	1.81	0.10	0
680	89.998	0.89998	0.005557902	4.40871E+14	1.82	0.10	0
675	90.031	0.90031	0.005519263	4.44137E+14	1.84	0.10	0
670	90.071	0.90071	0.005472629	4.47451E+14	1.85	0.10	0
665	90.105	0.90105	0.005433163	4.50816E+14	1.86	0.10	0
660	90.14	0.9014	0.0053927	4.54231E+14	1.88	0.10	0
655	90.16	0.9016	0.005369654	4.57698E+14	1.89	0.10	0
650	90.184	0.90184	0.00534207	4.61219E+14	1.91	0.10	0
645	90.202	0.90202	0.005321434	4.64795E+14	1.92	0.10	0
640	90.21	0.9021	0.005312277	4.68426E+14	1.94	0.10	0
635	90.179	0.90179	0.005347811	4.72114E+14	1.95	0.10	0
630	90.157	0.90157	0.005373107	4.75861E+14	1.97	0.10	0
625	90.169	0.90169	0.005359301	4.79668E+14	1.98	0.10	0
620	90.224	0.90224	0.005296272	4.83536E+14	2.00	0.10	0
615	90.222	0.90222	0.005298557	4.87467E+14	2.02	0.10	0
610	90.199	0.90199	0.005324871	4.91463E+14	2.03	0.10	0
605	90.163	0.90163	0.005366202	4.95525E+14	2.05	0.10	0
600	90.143	0.90143	0.00538924	4.99654E+14	2.07	0.11	0
595	90.115	0.90115	0.005421585	5.03853E+14	2.08	0.11	0
590	90.083	0.90083	0.005458682	5.08123E+14	2.10	0.11	0
585	90.038	0.90038	0.005511087	5.12466E+14	2.12	0.11	0
580	89.999	0.89999	0.005556728	5.16884E+14	2.14	0.11	0
575	89.951	0.89951	0.005613189	5.21378E+14	2.16	0.11	0

570	89.899	0.89899	0.005674713	5.25952E+14	2.18	0.11	0
565	89.847	0.89847	0.005736608	5.30606E+14	2.19	0.11	0
560	89.789	0.89789	0.005806085	5.35344E+14	2.21	0.11	0
555	89.734	0.89734	0.005872398	5.40167E+14	2.23	0.11	0
550	89.664	0.89664	0.005957402	5.45077E+14	2.25	0.12	0
545	89.609	0.89609	0.006024667	5.50078E+14	2.27	0.12	0
540	89.542	0.89542	0.006107177	5.55171E+14	2.30	0.12	0
535	89.508	0.89508	0.006149286	5.6036E+14	2.32	0.12	0
530	89.439	0.89439	0.00623524	5.65646E+14	2.34	0.12	0
525	89.38	0.8938	0.006309264	5.71033E+14	2.36	0.12	0
520	89.322	0.89322	0.006382508	5.76524E+14	2.38	0.12	0
515	89.25	0.8925	0.00647409	5.82121E+14	2.41	0.12	0
510	89.165	0.89165	0.006583145	5.87828E+14	2.43	0.13	0
505	89.058	0.89058	0.006721876	5.93648E+14	2.46	0.13	0
500	88.977	0.88977	0.006827974	5.99585E+14	2.48	0.13	0
495	88.889	0.88889	0.006944297	6.05641E+14	2.50	0.13	0
490	88.785	0.88785	0.007083191	6.11821E+14	2.53	0.13	0
485	88.664	0.88664	0.007246735	6.18129E+14	2.56	0.14	0
480	88.551	0.88551	0.007401362	6.24568E+14	2.58	0.14	0
475	88.435	0.88435	0.007562007	6.31142E+14	2.61	0.14	0
470	88.295	0.88295	0.007758482	6.37856E+14	2.64	0.14	0
465	88.152	0.88152	0.007962105	6.44715E+14	2.67	0.15	0
460	88.002	0.88002	0.008178905	6.51723E+14	2.70	0.15	0
455	87.851	0.87851	0.008400485	6.58885E+14	2.72	0.15	0
450	87.679	0.87679	0.008656978	6.66205E+14	2.76	0.15	0
445	87.485	0.87485	0.008951547	6.73691E+14	2.79	0.16	0
440	87.268	0.87268	0.009287701	6.81346E+14	2.82	0.16	0
435	86.992	0.86992	0.009725496	6.89178E+14	2.85	0.17	0
430	86.694	0.86694	0.010211182	6.97192E+14	2.88	0.17	0
425	86.34	0.8634	0.010805861	7.05394E+14	2.92	0.18	0
420	85.858	0.85858	0.011646915	7.13792E+14	2.95	0.19	0
415	85.191	0.85191	0.012871458	7.22391E+14	2.99	0.20	0
410	84.248	0.84248	0.014725899	7.31201E+14	3.02	0.21	0
405	82.846	0.82846	0.01775944	7.40228E+14	3.06	0.23	0
400	80.637	0.80637	0.02324775	7.49481E+14	3.10	0.27	0
395	77.121	0.77121	0.033936842	7.58968E+14	3.14	0.33	0
390	71.663	0.71663	0.056025115	7.68699E+14	3.18	0.42	0.001
385	63.817	0.63817	0.102575293	7.78682E+14	3.22	0.57	0.001
380	53.886	0.53886	0.197314794	7.88928E+14	3.26	0.80	0.002
375	42.836	0.42836	0.381422506	7.99447E+14	3.31	1.12	0.004
370	32.079	0.32079	0.719047078	8.1025E+14	3.35	1.55	0.007
365	22.824	0.22824	1.304796481	8.21349E+14	3.40	2.11	0.013
360	15.851	0.15851	2.233630118	8.32757E+14	3.44	2.77	0.022
355	11.272	0.11272	3.49213005	8.44486E+14	3.49	3.49	0.035
350	8.582	0.08582	4.869057751	8.56555E+14	3.54	4.15	0.049
345	7.074	0.07074	6.103506839	8.68964E+14	3.59	4.68	0.061
340	6.215	0.06215	7.076127293	8.81743E+14	3.65	5.08	0.071
335	5.772	0.05772	7.691368663	8.94903E+14	3.70	5.34	0.077
330	5.598	0.05598	7.959751343	9.08462E+14	3.76	5.47	0.08
325	5.542	0.05542	8.049723713	9.22438E+14	3.81	5.54	0.08
320	5.537	0.05537	8.057845737	9.36851E+14	3.87	5.59	0.081
315	5.553	0.05553	8.031906905	9.51722E+14	3.94	5.62	0.08
310	5.573	0.05573	7.999693459	9.67072E+14	4.00	5.66	0.08
305	5.629	0.05629	7.910717393	9.82926E+14	4.07	5.67	0.079
300	5.73	0.0573	7.75465349	9.99308E+14	4.13	5.66	0.078
295	5.861	0.05861	7.560272412	1.01625E+15	4.20	5.64	0.076

290	5.984	0.05984	7.385534973	1.03377E+15	4.28	5.62	0.074
285	6.071	0.06071	7.266230474	1.0519E+15	4.35	5.62	0.073
280	6.131	0.06131	7.185931464	1.07069E+15	4.43	5.64	0.072
275	6.166	0.06166	7.139814755	1.09015E+15	4.51	5.67	0.071
270	6.195	0.06195	7.10200002	1.11034E+15	4.59	5.71	0.071
265	6.213	0.06213	7.078707041	1.13129E+15	4.68	5.75	0.071
260	6.198	0.06198	7.098108425	1.15305E+15	4.77	5.82	0.071
255	6.131	0.06131	7.185931464	1.17566E+15	4.86	5.91	0.072
250	5.997	0.05997	7.367487084	1.19917E+15	4.96	6.04	0.074
245	5.823	0.05823	7.615754189	1.22364E+15	5.06	6.21	0.076
240	5.647	0.05647	7.882493899	1.24914E+15	5.17	6.38	0.079
235	5.493	0.05493	8.129959083	1.27571E+15	5.28	6.55	0.081
230	5.383	0.05383	8.315415836	1.30345E+15	5.39	6.70	0.083
225	5.304	0.05304	8.453367662	1.33241E+15	5.51	6.83	0.085
220	5.273	0.05273	8.508633159	1.36269E+15	5.64	6.92	0.085
215	5.267	0.05267	8.519405059	1.39438E+15	5.77	7.01	0.085
210	5.309	0.05309	8.444514486	1.42758E+15	5.90	7.06	0.084
205	5.38	0.0538	8.320580297	1.4624E+15	6.05	7.09	0.083
200	5.469	0.05469	8.169784203	1.49896E+15	6.20	7.12	0.082

Table 2: Impregnation 10%

10% ZnTiO2 (Impregnation)							
wavelength	% Reflectance	Reflectance	F(R)=(1-R)^2/(2R)	v=c/wavelength	E=hv	sqrt(F(R)*E)	Absorbance
800	90.216	0.90216	0.005305415	3.74741E+14	1.55	0.09	0
795	90.256	0.90256	0.005259791	3.77097E+14	1.56	0.09	0
790	90.265	0.90265	0.005249555	3.79484E+14	1.57	0.09	0
785	90.279	0.90279	0.005233656	3.81901E+14	1.58	0.09	0
780	90.259	0.90259	0.005256378	3.84349E+14	1.59	0.09	0
775	90.221	0.90221	0.0052997	3.86829E+14	1.60	0.09	0
770	90.204	0.90204	0.005319144	3.89341E+14	1.61	0.09	0
765	90.179	0.90179	0.005347811	3.91886E+14	1.62	0.09	0
760	90.196	0.90196	0.005328308	3.94464E+14	1.63	0.09	0
755	90.202	0.90202	0.005321434	3.97076E+14	1.64	0.09	0
750	90.175	0.90175	0.005352405	3.99723E+14	1.65	0.09	0
745	90.164	0.90164	0.005365051	4.02406E+14	1.66	0.09	0
740	90.175	0.90175	0.005352405	4.05125E+14	1.68	0.09	0
735	90.172	0.90172	0.005355852	4.07881E+14	1.69	0.10	0
730	90.164	0.90164	0.005365051	4.10675E+14	1.70	0.10	0
725	90.157	0.90157	0.005373107	4.13507E+14	1.71	0.10	0
720	90.143	0.90143	0.00538924	4.16378E+14	1.72	0.10	0
715	90.121	0.90121	0.005414645	4.1929E+14	1.73	0.10	0
710	90.12	0.9012	0.005415801	4.22243E+14	1.75	0.10	0
705	90.137	0.90137	0.005396162	4.25238E+14	1.76	0.10	0
700	90.137	0.90137	0.005396162	4.28275E+14	1.77	0.10	0
695	90.144	0.90144	0.005388087	4.31356E+14	1.78	0.10	0
690	90.175	0.90175	0.005352405	4.34482E+14	1.80	0.10	0
685	90.215	0.90215	0.005306558	4.37653E+14	1.81	0.10	0
680	90.253	0.90253	0.005263205	4.40871E+14	1.82	0.10	0
675	90.262	0.90262	0.005252966	4.44137E+14	1.84	0.10	0
670	90.277	0.90277	0.005235925	4.47451E+14	1.85	0.10	0
665	90.32	0.9032	0.005187245	4.50816E+14	1.86	0.10	0
660	90.353	0.90353	0.005150056	4.54231E+14	1.88	0.10	0
655	90.384	0.90384	0.005115256	4.57698E+14	1.89	0.10	0
650	90.392	0.90392	0.005106296	4.61219E+14	1.91	0.10	0
645	90.396	0.90396	0.00510182	4.64795E+14	1.92	0.10	0
640	90.381	0.90381	0.005118618	4.68426E+14	1.94	0.10	0
635	90.331	0.90331	0.005174833	4.72114E+14	1.95	0.10	0
630	90.308	0.90308	0.005200805	4.75861E+14	1.97	0.10	0
625	90.312	0.90312	0.005196283	4.79668E+14	1.98	0.10	0
620	90.373	0.90373	0.005127589	4.83536E+14	2.00	0.10	0
615	90.379	0.90379	0.00512086	4.87467E+14	2.02	0.10	0
610	90.347	0.90347	0.005156807	4.91463E+14	2.03	0.10	0
605	90.302	0.90302	0.005207593	4.95525E+14	2.05	0.10	0
600	90.262	0.90262	0.005252966	4.99654E+14	2.07	0.10	0
595	90.222	0.90222	0.005298557	5.03853E+14	2.08	0.11	0
590	90.182	0.90182	0.005344366	5.08123E+14	2.10	0.11	0
585	90.14	0.9014	0.0053927	5.12466E+14	2.12	0.11	0
580	90.086	0.90086	0.005455198	5.16884E+14	2.14	0.11	0
575	90.031	0.90031	0.005519263	5.21378E+14	2.16	0.11	0
570	89.972	0.89972	0.005588449	5.25952E+14	2.18	0.11	0
565	89.903	0.89903	0.005669967	5.30606E+14	2.19	0.11	0
560	89.838	0.89838	0.005747359	5.35344E+14	2.21	0.11	0
555	89.76	0.8976	0.005840998	5.40167E+14	2.23	0.11	0

550	89.677	0.89677	0.005941564	5.45077E+14	2.25	0.12	0
545	89.607	0.89607	0.006027121	5.50078E+14	2.27	0.12	0
540	89.54	0.8954	0.006109649	5.55171E+14	2.30	0.12	0
535	89.485	0.89485	0.006177864	5.6036E+14	2.32	0.12	0
530	89.415	0.89415	0.006265292	5.65646E+14	2.34	0.12	0
525	89.333	0.89333	0.006368581	5.71033E+14	2.36	0.12	0
520	89.261	0.89261	0.006460051	5.76524E+14	2.38	0.12	0
515	89.157	0.89157	0.006593461	5.82121E+14	2.41	0.13	0
510	89.056	0.89056	0.006724484	5.87828E+14	2.43	0.13	0
505	88.934	0.88934	0.006884676	5.93648E+14	2.46	0.13	0
500	88.829	0.88829	0.00702424	5.99585E+14	2.48	0.13	0
495	88.707	0.88707	0.007188376	6.05641E+14	2.50	0.13	0
490	88.573	0.88573	0.007371114	6.11821E+14	2.53	0.14	0
485	88.429	0.88429	0.00757037	6.18129E+14	2.56	0.14	0
480	88.292	0.88292	0.007762723	6.24568E+14	2.58	0.14	0
475	88.141	0.88141	0.007977892	6.31142E+14	2.61	0.14	0
470	87.964	0.87964	0.008234351	6.37856E+14	2.64	0.15	0
465	87.79	0.8779	0.00849095	6.44715E+14	2.67	0.15	0
460	87.576	0.87576	0.008812676	6.51723E+14	2.70	0.15	0
455	87.347	0.87347	0.009164505	6.58885E+14	2.72	0.16	0
450	87.085	0.87085	0.009576691	6.66205E+14	2.76	0.16	0
445	86.777	0.86777	0.010074543	6.73691E+14	2.79	0.17	0
440	86.411	0.86411	0.010685036	6.81346E+14	2.82	0.17	0
435	85.968	0.85968	0.011451763	6.89178E+14	2.85	0.18	0
430	85.466	0.85466	0.012357964	6.97192E+14	2.88	0.19	0
425	84.877	0.84877	0.013472739	7.05394E+14	2.92	0.20	0
420	84.14	0.8414	0.014947682	7.13792E+14	2.95	0.21	0
415	83.17	0.8317	0.017028309	7.22391E+14	2.99	0.23	0
410	81.889	0.81889	0.020027618	7.31201E+14	3.02	0.25	0
405	80.136	0.80136	0.024619303	7.40228E+14	3.06	0.27	0
400	77.592	0.77592	0.03235633	7.49481E+14	3.10	0.32	0
395	73.845	0.73845	0.046318913	7.58968E+14	3.14	0.38	0
390	68.326	0.68326	0.07341585	7.68699E+14	3.18	0.48	0.001
385	60.767	0.60767	0.126650015	7.78682E+14	3.22	0.64	0.001
380	51.52	0.5152	0.228096894	7.88928E+14	3.26	0.86	0.002
375	41.464	0.41464	0.413185329	7.99447E+14	3.31	1.17	0.004
370	31.725	0.31725	0.734669129	8.1025E+14	3.35	1.57	0.007
365	23.247	0.23247	1.267050159	8.21349E+14	3.40	2.07	0.013
360	16.676	0.16676	2.08170094	8.32757E+14	3.44	2.68	0.021
355	12.228	0.12228	3.15011612	8.44486E+14	3.49	3.32	0.031
350	9.492	0.09492	4.315053763	8.56555E+14	3.54	3.91	0.043
345	7.951	0.07951	5.328272168	8.68964E+14	3.59	4.38	0.053
340	7.013	0.07013	6.164681427	8.81743E+14	3.65	4.74	0.062
335	6.538	0.06538	6.680288654	8.94903E+14	3.70	4.97	0.067
330	6.34	0.0634	6.918135331	9.08462E+14	3.76	5.10	0.069
325	6.261	0.06261	7.017249737	9.22438E+14	3.81	5.17	0.07
320	6.256	0.06256	7.023607366	9.36851E+14	3.87	5.22	0.07
315	6.239	0.06239	7.045299824	9.51722E+14	3.94	5.27	0.07
310	6.271	0.06271	7.004565014	9.67072E+14	4.00	5.29	0.07
305	6.334	0.06334	6.925575905	9.82926E+14	4.07	5.31	0.069
300	6.448	0.06448	6.786582432	9.99308E+14	4.13	5.30	0.068
295	6.589	0.06589	6.621349917	1.01625E+15	4.20	5.28	0.066
290	6.731	0.06731	6.461971743	1.03377E+15	4.28	5.26	0.065
285	6.836	0.06836	6.348398841	1.0519E+15	4.35	5.26	0.063
280	6.902	0.06902	6.278787021	1.07069E+15	4.43	5.27	0.063
275	6.941	0.06941	6.238277972	1.09015E+15	4.51	5.30	0.062

270	6.972	0.06972	6.206403316	1.11034E+15	4.59	5.34	0.062
265	6.99	0.0699	6.188025823	1.13129E+15	4.68	5.38	0.062
260	6.979	0.06979	6.199245193	1.15305E+15	4.77	5.44	0.062
255	6.903	0.06903	6.277742582	1.17566E+15	4.86	5.52	0.063
250	6.757	0.06757	6.43351861	1.19917E+15	4.96	5.65	0.064
245	6.558	0.06558	6.657065694	1.22364E+15	5.06	5.80	0.067
240	6.358	0.06358	6.89589821	1.24914E+15	5.17	5.97	0.069
235	6.195	0.06195	7.10200002	1.27571E+15	5.28	6.12	0.071
230	6.071	0.06071	7.266230474	1.30345E+15	5.39	6.26	0.073
225	5.989	0.05989	7.378584172	1.33241E+15	5.51	6.38	0.074
220	5.928	0.05928	7.464187908	1.36269E+15	5.64	6.49	0.075
215	5.917	0.05917	7.479813156	1.39438E+15	5.77	6.57	0.075
210	5.959	0.05959	7.420464575	1.42758E+15	5.90	6.62	0.074
205	6.046	0.06046	7.300160533	1.4624E+15	6.05	6.64	0.073
200	6.149	0.06149	7.16214848	1.49896E+15	6.20	6.66	0.072

Table 3: Impregnation 15%

15% ZnTiO2 (Impregnation)							
wavelength	% Reflectance	Reflectance	F(R)=(1-R)^2/(2R)	v=c/wavelength	E=hv	sqrt(F(R)*E)	Absorbance
800	97.893	0.97893	0.00022675	3.74741E+14	1.55	0.02	0
795	97.903	0.97903	0.00022458	3.77097E+14	1.56	0.02	0
790	97.894	0.97894	0.000226533	3.79484E+14	1.57	0.02	0
785	97.94	0.9794	0.000216643	3.81901E+14	1.58	0.02	0
780	97.903	0.97903	0.00022458	3.84349E+14	1.59	0.02	0
775	97.842	0.97842	0.000237984	3.86829E+14	1.60	0.02	0
770	97.812	0.97812	0.000244722	3.89341E+14	1.61	0.02	0
765	97.8	0.978	0.000247444	3.91886E+14	1.62	0.02	0
760	97.815	0.97815	0.000244044	3.94464E+14	1.63	0.02	0
755	97.798	0.97798	0.000247899	3.97076E+14	1.64	0.02	0
750	97.768	0.97768	0.000254778	3.99723E+14	1.65	0.02	0
745	97.746	0.97746	0.000259884	4.02406E+14	1.66	0.02	0
740	97.751	0.97751	0.000258719	4.05125E+14	1.68	0.02	0
735	97.737	0.97737	0.000261987	4.07881E+14	1.69	0.02	0
730	97.755	0.97755	0.000257789	4.10675E+14	1.70	0.02	0
725	97.716	0.97716	0.000266929	4.13507E+14	1.71	0.02	0
720	97.696	0.97696	0.000271168	4.16378E+14	1.72	0.02	0
715	97.664	0.97664	0.000279371	4.1929E+14	1.73	0.02	0
710	97.673	0.97673	0.000277197	4.22243E+14	1.75	0.02	0
705	97.687	0.97687	0.000273832	4.25238E+14	1.76	0.02	0
700	97.694	0.97694	0.000272158	4.28275E+14	1.77	0.02	0
695	97.69	0.9769	0.000273114	4.31356E+14	1.78	0.02	0
690	97.731	0.97731	0.000263394	4.34482E+14	1.80	0.02	0
685	97.763	0.97763	0.000255934	4.37653E+14	1.81	0.02	0
680	97.803	0.97803	0.000246762	4.40871E+14	1.82	0.02	0
675	97.818	0.97818	0.000243366	4.44137E+14	1.84	0.02	0
670	97.821	0.97821	0.00024269	4.47451E+14	1.85	0.02	0
665	97.862	0.97862	0.000233545	4.50816E+14	1.86	0.02	0
660	97.885	0.97885	0.000228494	4.54231E+14	1.88	0.02	0
655	97.922	0.97922	0.000220486	4.57698E+14	1.89	0.02	0
650	97.929	0.97929	0.000218987	4.61219E+14	1.91	0.02	0
645	97.945	0.97945	0.000215581	4.64795E+14	1.92	0.02	0
640	97.951	0.97951	0.000214311	4.68426E+14	1.94	0.02	0
635	97.931	0.97931	0.00021856	4.72114E+14	1.95	0.02	0
630	97.905	0.97905	0.000224147	4.75861E+14	1.97	0.02	0
625	97.881	0.97881	0.000229368	4.79668E+14	1.98	0.02	0
620	97.897	0.97897	0.000225881	4.83536E+14	2.00	0.02	0
615	97.888	0.97888	0.000227839	4.87467E+14	2.02	0.02	0
610	97.862	0.97862	0.000233545	4.91463E+14	2.03	0.02	0
605	97.82	0.9782	0.000242916	4.95525E+14	2.05	0.02	0
600	97.781	0.97781	0.000251785	4.99654E+14	2.07	0.02	0
595	97.728	0.97728	0.0002641	5.03853E+14	2.08	0.02	0
590	97.675	0.97675	0.000276715	5.08123E+14	2.10	0.02	0
585	97.604	0.97604	0.000294087	5.12466E+14	2.12	0.02	0
580	97.534	0.97534	0.000311745	5.16884E+14	2.14	0.03	0
575	97.452	0.97452	0.000333103	5.21378E+14	2.16	0.03	0
570	97.375	0.97375	0.000353819	5.25952E+14	2.18	0.03	0
565	97.299	0.97299	0.000374896	5.30606E+14	2.19	0.03	0
560	97.22	0.9722	0.00039747	5.35344E+14	2.21	0.03	0
555	97.133	0.97133	0.000423115	5.40167E+14	2.23	0.03	0

550	97.046	0.97046	0.000449587	5.45077E+14	2.25	0.03	0
545	96.95	0.9695	0.000479758	5.50078E+14	2.27	0.03	0
540	96.854	0.96854	0.00051094	5.55171E+14	2.30	0.03	0
535	96.776	0.96776	0.000537022	5.6036E+14	2.32	0.04	0
530	96.675	0.96675	0.000571793	5.65646E+14	2.34	0.04	0
525	96.565	0.96565	0.000610947	5.71033E+14	2.36	0.04	0
520	96.454	0.96454	0.000651819	5.76524E+14	2.38	0.04	0
515	96.332	0.96332	0.000698326	5.82121E+14	2.41	0.04	0
510	96.211	0.96211	0.000746096	5.87828E+14	2.43	0.04	0
505	96.063	0.96063	0.000806761	5.93648E+14	2.46	0.04	0
500	95.923	0.95923	0.00086642	5.99585E+14	2.48	0.05	0
495	95.753	0.95753	0.000941851	6.05641E+14	2.50	0.05	0
490	95.599	0.95599	0.001013023	6.11821E+14	2.53	0.05	0
485	95.419	0.95419	0.001099653	6.18129E+14	2.56	0.05	0
480	95.224	0.95224	0.001197712	6.24568E+14	2.58	0.06	0
475	95.01	0.9501	0.001310394	6.31142E+14	2.61	0.06	0
470	94.733	0.94733	0.001464183	6.37856E+14	2.64	0.06	0
465	94.456	0.94456	0.001626998	6.44715E+14	2.67	0.07	0
460	94.128	0.94128	0.001831569	6.51723E+14	2.70	0.07	0
455	93.768	0.93768	0.002070953	6.58885E+14	2.72	0.08	0
450	93.346	0.93346	0.002371591	6.66205E+14	2.76	0.08	0
445	92.863	0.92863	0.002742576	6.73691E+14	2.79	0.09	0
440	92.316	0.92316	0.003197921	6.81346E+14	2.82	0.09	0
435	91.67	0.9167	0.003784711	6.89178E+14	2.85	0.10	0
430	90.933	0.90933	0.004520388	6.97192E+14	2.88	0.11	0
425	90.047	0.90047	0.005500584	7.05394E+14	2.92	0.13	0
420	89.005	0.89005	0.006791193	7.13792E+14	2.95	0.14	0
415	87.706	0.87706	0.008616425	7.22391E+14	2.99	0.16	0
410	86.081	0.86081	0.011253271	7.31201E+14	3.02	0.18	0
405	83.972	0.83972	0.015296574	7.40228E+14	3.06	0.22	0
400	81.151	0.81151	0.021890353	7.49481E+14	3.10	0.26	0
395	77.26	0.7726	0.033465415	7.58968E+14	3.14	0.32	0
390	71.805	0.71805	0.055355339	7.68699E+14	3.18	0.42	0.001
385	64.427	0.64427	0.098207144	7.78682E+14	3.22	0.56	0.001
380	55.298	0.55298	0.180681833	7.88928E+14	3.26	0.77	0.002
375	45.096	0.45096	0.334225787	7.99447E+14	3.31	1.05	0.003
370	34.898	0.34898	0.607236862	8.1025E+14	3.35	1.43	0.006
365	25.742	0.25742	1.071061022	8.21349E+14	3.40	1.91	0.011
360	18.512	0.18512	1.793510735	8.32757E+14	3.44	2.49	0.018
355	13.536	0.13536	2.761533428	8.44486E+14	3.49	3.11	0.028
350	10.46	0.1046	3.832414723	8.56555E+14	3.54	3.68	0.038
345	8.693	0.08693	4.795219285	8.68964E+14	3.59	4.15	0.048
340	7.623	0.07623	5.597212468	8.81743E+14	3.65	4.52	0.056
335	7.039	0.07039	6.138476716	8.94903E+14	3.70	4.77	0.061
330	6.786	0.06786	6.402040816	9.08462E+14	3.76	4.90	0.064
325	6.691	0.06691	6.506179555	9.22438E+14	3.81	4.98	0.065
320	6.664	0.06664	6.5363212	9.36851E+14	3.87	5.03	0.065
315	6.647	0.06647	6.555425462	9.51722E+14	3.94	5.08	0.066
310	6.674	0.06674	6.525129065	9.67072E+14	4.00	5.11	0.065
305	6.735	0.06735	6.457579974	9.82926E+14	4.07	5.12	0.065
300	6.854	0.06854	6.329280213	9.99308E+14	4.13	5.11	0.063
295	7.013	0.07013	6.164681427	1.01625E+15	4.20	5.09	0.062
290	7.161	0.07161	6.018070047	1.03377E+15	4.28	5.07	0.06
285	7.272	0.07272	5.912047569	1.0519E+15	4.35	5.07	0.059
280	7.346	0.07346	5.843155265	1.07069E+15	4.43	5.09	0.058
275	7.39	0.0739	5.802849865	1.09015E+15	4.51	5.11	0.058

270	7.423	0.07423	5.772936097	1.11034E+15	4.59	5.15	0.058
265	7.443	0.07443	5.754936349	1.13129E+15	4.68	5.19	0.058
260	7.428	0.07428	5.768427022	1.15305E+15	4.77	5.24	0.058
255	7.347	0.07347	5.842233843	1.17566E+15	4.86	5.33	0.058
250	7.196	0.07196	5.984284614	1.19917E+15	4.96	5.45	0.06
245	6.995	0.06995	6.182937831	1.22364E+15	5.06	5.59	0.062
240	6.784	0.06784	6.404203019	1.24914E+15	5.17	5.75	0.064
235	6.61	0.0661	6.59734652	1.27571E+15	5.28	5.90	0.066
230	6.487	0.06487	6.740158139	1.30345E+15	5.39	6.03	0.067
225	6.401	0.06401	6.843284488	1.33241E+15	5.51	6.14	0.068
220	6.354	0.06354	6.900828861	1.36269E+15	5.64	6.24	0.069
215	6.34	0.0634	6.918135331	1.39438E+15	5.77	6.32	0.069
210	6.4	0.064	6.8445	1.42758E+15	5.90	6.36	0.068
205	6.497	0.06497	6.728344628	1.4624E+15	6.05	6.38	0.067
200	6.615	0.06615	6.591653987	1.49896E+15	6.20	6.39	0.066

Table 4: Reflux 1:1mol ratio

1:1 Zn-TiO2 (Reflux)							
wavelength	% Reflectance	Reflectance	F(R)=(1-R)^2/(2R)	v=c/wavelength	E=hv	sqrt(F(R)*E)	Absorbance
800	90.239	0.90239	0.005279154	3.74741E+14	1.55	0.09	0
795	90.215	0.90215	0.005306558	3.77097E+14	1.56	0.09	0
790	90.164	0.90164	0.005365051	3.79484E+14	1.57	0.09	0
785	90.154	0.90154	0.005376562	3.81901E+14	1.58	0.09	0
780	90.134	0.90134	0.005399625	3.84349E+14	1.59	0.09	0
775	90.109	0.90109	0.00542853	3.86829E+14	1.60	0.09	0
770	90.108	0.90108	0.005429688	3.89341E+14	1.61	0.09	0
765	90.082	0.90082	0.005459843	3.91886E+14	1.62	0.09	0
760	90.096	0.90096	0.005443594	3.94464E+14	1.63	0.09	0
755	90.089	0.90089	0.005451716	3.97076E+14	1.64	0.09	0
750	90.082	0.90082	0.005459843	3.99723E+14	1.65	0.10	0
745	90.065	0.90065	0.005479611	4.02406E+14	1.66	0.10	0
740	90.085	0.90085	0.005456359	4.05125E+14	1.68	0.10	0
735	90.077	0.90077	0.005465653	4.07881E+14	1.69	0.10	0
730	90.071	0.90071	0.005472629	4.10675E+14	1.70	0.10	0
725	90.057	0.90057	0.005488926	4.13507E+14	1.71	0.10	0
720	90.044	0.90044	0.005504083	4.16378E+14	1.72	0.10	0
715	90.041	0.90041	0.005507584	4.1929E+14	1.73	0.10	0
710	90.034	0.90034	0.005515758	4.22243E+14	1.75	0.10	0
705	90.059	0.90059	0.005486597	4.25238E+14	1.76	0.10	0
700	90.08	0.9008	0.005462167	4.28275E+14	1.77	0.10	0
695	90.086	0.90086	0.005455198	4.31356E+14	1.78	0.10	0
690	90.121	0.90121	0.005414645	4.34482E+14	1.80	0.10	0
685	90.147	0.90147	0.005384628	4.37653E+14	1.81	0.10	0
680	90.166	0.90166	0.005362751	4.40871E+14	1.82	0.10	0
675	90.144	0.90144	0.005388087	4.44137E+14	1.84	0.10	0
670	90.137	0.90137	0.005396162	4.47451E+14	1.85	0.10	0
665	90.164	0.90164	0.005365051	4.50816E+14	1.86	0.10	0
660	90.192	0.90192	0.005332893	4.54231E+14	1.88	0.10	0
655	90.233	0.90233	0.005285998	4.57698E+14	1.89	0.10	0
650	90.259	0.90259	0.005256378	4.61219E+14	1.91	0.10	0
645	90.282	0.90282	0.005230252	4.64795E+14	1.92	0.10	0
640	90.276	0.90276	0.005237061	4.68426E+14	1.94	0.10	0
635	90.233	0.90233	0.005285998	4.72114E+14	1.95	0.10	0
630	90.204	0.90204	0.005319144	4.75861E+14	1.97	0.10	0
625	90.224	0.90224	0.005296272	4.79668E+14	1.98	0.10	0
620	90.289	0.90289	0.005222315	4.83536E+14	2.00	0.10	0
615	90.32	0.9032	0.005187245	4.87467E+14	2.02	0.10	0
610	90.314	0.90314	0.005194023	4.91463E+14	2.03	0.10	0
605	90.295	0.90295	0.005215517	4.95525E+14	2.05	0.10	0
600	90.283	0.90283	0.005229118	4.99654E+14	2.07	0.10	0
595	90.277	0.90277	0.005235925	5.03853E+14	2.08	0.10	0
590	90.259	0.90259	0.005256378	5.08123E+14	2.10	0.11	0
585	90.233	0.90233	0.005285998	5.12466E+14	2.12	0.11	0
580	90.196	0.90196	0.005328308	5.16884E+14	2.14	0.11	0
575	90.154	0.90154	0.005376562	5.21378E+14	2.16	0.11	0
570	90.103	0.90103	0.00543548	5.25952E+14	2.18	0.11	0
565	90.054	0.90054	0.005492422	5.30606E+14	2.19	0.11	0
560	90.007	0.90007	0.005547349	5.35344E+14	2.21	0.11	0
555	89.952	0.89952	0.00561201	5.40167E+14	2.23	0.11	0

550	89.871	0.89871	0.005707995	5.45077E+14	2.25	0.11	0
545	89.79	0.8979	0.005804884	5.50078E+14	2.27	0.11	0
540	89.699	0.89699	0.005914815	5.55171E+14	2.30	0.12	0
535	89.632	0.89632	0.005996487	5.6036E+14	2.32	0.12	0
530	89.536	0.89536	0.006114596	5.65646E+14	2.34	0.12	0
525	89.441	0.89441	0.006232739	5.71033E+14	2.36	0.12	0
520	89.328	0.89328	0.00637491	5.76524E+14	2.38	0.12	0
515	89.189	0.89189	0.00655225	5.82121E+14	2.41	0.13	0
510	89.044	0.89044	0.006740147	5.87828E+14	2.43	0.13	0
505	88.873	0.88873	0.006965565	5.93648E+14	2.46	0.13	0
500	88.698	0.88698	0.007200568	5.99585E+14	2.48	0.13	0
495	88.484	0.88484	0.007493912	6.05641E+14	2.50	0.14	0
490	88.237	0.88237	0.007840711	6.11821E+14	2.53	0.14	0
485	87.956	0.87956	0.008246051	6.18129E+14	2.56	0.15	0
480	87.65	0.8765	0.008700656	6.24568E+14	2.58	0.15	0
475	87.314	0.87314	0.009215853	6.31142E+14	2.61	0.16	0
470	86.89	0.8689	0.009890212	6.37856E+14	2.64	0.16	0
465	86.411	0.86411	0.010685036	6.44715E+14	2.67	0.17	0
460	85.835	0.85835	0.011687961	6.51723E+14	2.70	0.18	0
455	85.193	0.85193	0.01286768	6.58885E+14	2.72	0.19	0
450	84.445	0.84445	0.014326368	6.66205E+14	2.76	0.20	0
445	83.594	0.83594	0.016099052	6.73691E+14	2.79	0.21	0
440	82.622	0.82622	0.018275694	6.81346E+14	2.82	0.23	0
435	81.522	0.81522	0.020941371	6.89178E+14	2.85	0.24	0
430	80.321	0.80321	0.02410721	6.97192E+14	2.88	0.26	0
425	78.984	0.78984	0.027959603	7.05394E+14	2.92	0.29	0
420	77.477	0.77477	0.032737814	7.13792E+14	2.95	0.31	0
415	75.766	0.75766	0.038756616	7.22391E+14	2.99	0.34	0
410	73.811	0.73811	0.046460807	7.31201E+14	3.02	0.37	0
405	71.49	0.7149	0.056848517	7.40228E+14	3.06	0.42	0.001
400	68.613	0.68613	0.071789877	7.49481E+14	3.10	0.47	0.001
395	64.865	0.64865	0.095156727	7.58968E+14	3.14	0.55	0.001
390	59.85	0.5985	0.134671888	7.68699E+14	3.18	0.65	0.001
385	53.273	0.53273	0.204926748	7.78682E+14	3.22	0.81	0.002
380	45.308	0.45308	0.330097871	7.88928E+14	3.26	1.04	0.003
375	36.523	0.36523	0.551615356	7.99447E+14	3.31	1.35	0.006
370	27.829	0.27829	0.935831909	8.1025E+14	3.35	1.77	0.009
365	20.157	0.20157	1.581312856	8.21349E+14	3.40	2.32	0.016
360	14.227	0.14227	2.585579366	8.32757E+14	3.44	2.98	0.026
355	10.236	0.10236	3.935900594	8.44486E+14	3.49	3.71	0.039
350	7.845	0.07845	5.412711297	8.56555E+14	3.54	4.38	0.054
345	6.508	0.06508	6.715391875	8.68964E+14	3.59	4.91	0.067
340	5.73	0.0573	7.75465349	8.81743E+14	3.65	5.32	0.078
335	5.331	0.05331	8.405758358	8.94903E+14	3.70	5.58	0.084
330	5.151	0.05151	8.732608038	9.08462E+14	3.76	5.73	0.087
325	5.098	0.05098	8.833257752	9.22438E+14	3.81	5.80	0.088
320	5.101	0.05101	8.827504608	9.36851E+14	3.87	5.85	0.088
315	5.086	0.05086	8.856338376	9.51722E+14	3.94	5.90	0.089
310	5.104	0.05104	8.821758245	9.67072E+14	4.00	5.94	0.088
305	5.144	0.05144	8.745782208	9.82926E+14	4.07	5.96	0.087
300	5.243	0.05243	8.56273989	9.99308E+14	4.13	5.95	0.086
295	5.359	0.05359	8.356893899	1.01625E+15	4.20	5.93	0.084
290	5.475	0.05475	8.159795091	1.03377E+15	4.28	5.91	0.082
285	5.56	0.0556	8.020605755	1.0519E+15	4.35	5.91	0.08
280	5.617	0.05617	7.92963387	1.07069E+15	4.43	5.93	0.079
275	5.652	0.05652	7.874686044	1.09015E+15	4.51	5.96	0.079

270	5.681	0.05681	7.829672383	1.11034E+15	4.59	6.00	0.078
265	5.704	0.05704	7.794298401	1.13129E+15	4.68	6.04	0.078
260	5.701	0.05701	7.798896159	1.15305E+15	4.77	6.10	0.078
255	5.647	0.05647	7.882493899	1.17566E+15	4.86	6.19	0.079
250	5.542	0.05542	8.049723713	1.19917E+15	4.96	6.32	0.08
245	5.4	0.054	8.286259259	1.22364E+15	5.06	6.48	0.083
240	5.249	0.05249	8.551868928	1.24914E+15	5.17	6.65	0.086
235	5.124	0.05124	8.783621561	1.27571E+15	5.28	6.81	0.088
230	5.037	0.05037	8.951728578	1.30345E+15	5.39	6.95	0.09
225	4.982	0.04982	9.061040068	1.33241E+15	5.51	7.07	0.091
220	4.959	0.04959	9.107472959	1.36269E+15	5.64	7.16	0.091
215	4.951	0.04951	9.123724905	1.39438E+15	5.77	7.25	0.091
210	5.016	0.05016	8.993182073	1.42758E+15	5.90	7.29	0.09
205	5.106	0.05106	8.817931097	1.4624E+15	6.05	7.30	0.088
200	5.234	0.05234	8.579093194	1.49896E+15	6.20	7.29	0.086

Table 5: Reflux 1:2 mol ratio

1:2 Zn-TiO2 (Reflux)							
wavelength	% Reflectance	Reflectance	F(R)=(1-R)^2/(2R)	v=c/wavelength	E=hv	sqrt(F(R)*E)	Absorbance
800	97.69	0.9769	0.000273114	3.74741E+14	1.55	0.02	0
795	97.675	0.97675	0.000276715	3.77097E+14	1.56	0.02	0
790	97.627	0.97627	0.0002884	3.79484E+14	1.57	0.02	0
785	97.643	0.97643	0.000284478	3.81901E+14	1.58	0.02	0
780	97.595	0.97595	0.000296328	3.84349E+14	1.59	0.02	0
775	97.523	0.97523	0.000314568	3.86829E+14	1.60	0.02	0
770	97.461	0.97461	0.000330723	3.89341E+14	1.61	0.02	0
765	97.397	0.97397	0.000347835	3.91886E+14	1.62	0.02	0
760	97.362	0.97362	0.00035738	3.94464E+14	1.63	0.02	0
755	97.322	0.97322	0.000368451	3.97076E+14	1.64	0.02	0
750	97.264	0.97264	0.000384813	3.99723E+14	1.65	0.03	0
745	97.229	0.97229	0.000394864	4.02406E+14	1.66	0.03	0
740	97.189	0.97189	0.000406513	4.05125E+14	1.68	0.03	0
735	97.16	0.9716	0.000415068	4.07881E+14	1.69	0.03	0
730	97.121	0.97121	0.000426717	4.10675E+14	1.70	0.03	0
725	97.054	0.97054	0.000447118	4.13507E+14	1.71	0.03	0
720	96.985	0.96985	0.000468641	4.16378E+14	1.72	0.03	0
715	96.935	0.96935	0.000484563	4.1929E+14	1.73	0.03	0
710	96.895	0.96895	0.000497499	4.22243E+14	1.75	0.03	0
705	96.86	0.9686	0.000508961	4.25238E+14	1.76	0.03	0
700	96.819	0.96819	0.000522561	4.28275E+14	1.77	0.03	0
695	96.761	0.96761	0.000542115	4.31356E+14	1.78	0.03	0
690	96.733	0.96733	0.000551688	4.34482E+14	1.80	0.03	0
685	96.683	0.96683	0.000568998	4.37653E+14	1.81	0.03	0
680	96.625	0.96625	0.000589424	4.40871E+14	1.82	0.03	0
675	96.558	0.96558	0.000613484	4.44137E+14	1.84	0.03	0
670	96.472	0.96472	0.000645098	4.47451E+14	1.85	0.03	0
665	96.419	0.96419	0.000664991	4.50816E+14	1.86	0.04	0
660	96.365	0.96365	0.000685582	4.54231E+14	1.88	0.04	0
655	96.327	0.96327	0.000700267	4.57698E+14	1.89	0.04	0
650	96.284	0.96284	0.000717079	4.61219E+14	1.91	0.04	0
645	96.254	0.96254	0.000728932	4.64795E+14	1.92	0.04	0
640	96.214	0.96214	0.000744891	4.68426E+14	1.94	0.04	0
635	96.132	0.96132	0.000778171	4.72114E+14	1.95	0.04	0
630	96.031	0.96031	0.000820202	4.75861E+14	1.97	0.04	0
625	95.938	0.95938	0.000859922	4.79668E+14	1.98	0.04	0
620	95.877	0.95877	0.000886507	4.83536E+14	2.00	0.04	0
615	95.79	0.9579	0.000925154	4.87467E+14	2.02	0.04	0
610	95.691	0.95691	0.000970179	4.91463E+14	2.03	0.04	0
605	95.567	0.95567	0.001028152	4.95525E+14	2.05	0.05	0
600	95.451	0.95451	0.00108398	4.99654E+14	2.07	0.05	0
595	95.319	0.95319	0.001149391	5.03853E+14	2.08	0.05	0
590	95.163	0.95163	0.001229289	5.08123E+14	2.10	0.05	0
585	94.986	0.94986	0.001323363	5.12466E+14	2.12	0.05	0
580	94.766	0.94766	0.001445389	5.16884E+14	2.14	0.06	0
575	94.534	0.94534	0.001580233	5.21378E+14	2.16	0.06	0
570	94.284	0.94284	0.001732672	5.25952E+14	2.18	0.06	0
565	94.052	0.94052	0.001880806	5.30606E+14	2.19	0.06	0
560	93.846	0.93846	0.002017759	5.35344E+14	2.21	0.07	0
555	93.616	0.93616	0.002176736	5.40167E+14	2.23	0.07	0

550	93.37	0.9337	0.002353909	5.45077E+14	2.25	0.07	0
545	93.127	0.93127	0.002536221	5.50078E+14	2.27	0.08	0
540	92.885	0.92885	0.002725048	5.55171E+14	2.30	0.08	0
535	92.673	0.92673	0.002896471	5.6036E+14	2.32	0.08	0
530	92.448	0.92448	0.003084583	5.65646E+14	2.34	0.08	0
525	92.218	0.92218	0.003283498	5.71033E+14	2.36	0.09	0
520	91.98	0.9198	0.003496434	5.76524E+14	2.38	0.09	0
515	91.705	0.91705	0.003751542	5.82121E+14	2.41	0.10	0
510	91.412	0.91412	0.004034139	5.87828E+14	2.43	0.10	0
505	91.089	0.91089	0.0043587	5.93648E+14	2.46	0.10	0
500	90.765	0.90765	0.004698134	5.99585E+14	2.48	0.11	0
495	90.392	0.90392	0.005106296	6.05641E+14	2.50	0.11	0
490	89.996	0.89996	0.005560248	6.11821E+14	2.53	0.12	0
485	89.56	0.8956	0.006084949	6.18129E+14	2.56	0.12	0
480	89.093	0.89093	0.006676319	6.24568E+14	2.58	0.13	0
475	88.582	0.88582	0.007358759	6.31142E+14	2.61	0.14	0
470	87.979	0.87979	0.008212439	6.37856E+14	2.64	0.15	0
465	87.305	0.87305	0.009229885	6.44715E+14	2.67	0.16	0
460	86.528	0.86528	0.010487633	6.51723E+14	2.70	0.17	0
455	85.649	0.85649	0.012022978	6.58885E+14	2.72	0.18	0
450	84.648	0.84648	0.01392141	6.66205E+14	2.76	0.20	0
445	83.493	0.83493	0.016317598	6.73691E+14	2.79	0.21	0
440	82.17	0.8217	0.019344584	6.81346E+14	2.82	0.23	0
435	80.661	0.80661	0.023183256	6.89178E+14	2.85	0.26	0
430	78.963	0.78963	0.028022958	6.97192E+14	2.88	0.28	0
425	77.011	0.77011	0.034312898	7.05394E+14	2.92	0.32	0
420	74.789	0.74789	0.042492514	7.13792E+14	2.95	0.35	0
415	72.244	0.72244	0.053318998	7.22391E+14	2.99	0.40	0.001
410	69.395	0.69395	0.067488005	7.31201E+14	3.02	0.45	0.001
405	66.173	0.66173	0.086460182	7.40228E+14	3.06	0.51	0.001
400	62.494	0.62494	0.112546807	7.49481E+14	3.10	0.59	0.001
395	58.24	0.5824	0.149716484	7.58968E+14	3.14	0.69	0.001
390	53.282	0.53282	0.204813213	7.68699E+14	3.18	0.81	0.002
385	47.595	0.47595	0.288505518	7.78682E+14	3.22	0.96	0.003
380	41.316	0.41316	0.416764916	7.88928E+14	3.26	1.17	0.004
375	34.592	0.34592	0.618380907	7.99447E+14	3.31	1.43	0.006
370	27.713	0.27713	0.942772412	8.1025E+14	3.35	1.78	0.009
365	21.205	0.21205	1.463959449	8.21349E+14	3.40	2.23	0.015
360	15.749	0.15749	2.25354975	8.32757E+14	3.44	2.79	0.023
355	11.824	0.11824	3.287807415	8.44486E+14	3.49	3.39	0.033
350	9.29	0.0929	4.428581324	8.56555E+14	3.54	3.96	0.044
345	7.794	0.07794	5.454161173	8.68964E+14	3.59	4.43	0.055
340	6.863	0.06863	6.319758684	8.81743E+14	3.65	4.80	0.063
335	6.387	0.06387	6.86033644	8.94903E+14	3.70	5.04	0.069
330	6.139	0.06139	7.175343966	9.08462E+14	3.76	5.19	0.072
325	6.058	0.06058	7.283839026	9.22438E+14	3.81	5.27	0.073
320	6.021	0.06021	7.334373394	9.36851E+14	3.87	5.33	0.073
315	6.007	0.06007	7.35365744	9.51722E+14	3.94	5.38	0.074
310	6.013	0.06013	7.345381814	9.67072E+14	4.00	5.42	0.073
305	6.055	0.06055	7.287913315	9.82926E+14	4.07	5.44	0.073
300	6.152	0.06152	7.158198231	9.99308E+14	4.13	5.44	0.072
295	6.281	0.06281	6.991920841	1.01625E+15	4.20	5.42	0.07
290	6.401	0.06401	6.843284488	1.03377E+15	4.28	5.41	0.068
285	6.496	0.06496	6.729524335	1.0519E+15	4.35	5.41	0.067
280	6.554	0.06554	6.661698898	1.07069E+15	4.43	5.43	0.067
275	6.59	0.0659	6.620203414	1.09015E+15	4.51	5.46	0.066

270	6.615	0.06615	6.591653987	1.11034E+15	4.59	5.50	0.066
265	6.635	0.06635	6.568970026	1.13129E+15	4.68	5.54	0.066
260	6.625	0.06625	6.580294811	1.15305E+15	4.77	5.60	0.066
255	6.563	0.06563	6.651282164	1.17566E+15	4.86	5.69	0.067
250	6.445	0.06445	6.790176901	1.19917E+15	4.96	5.80	0.068
245	6.288	0.06288	6.983093944	1.22364E+15	5.06	5.94	0.07
240	6.133	0.06133	7.18328199	1.24914E+15	5.17	6.09	0.072
235	5.998	0.05998	7.366102037	1.27571E+15	5.28	6.23	0.074
230	5.904	0.05904	7.498354688	1.30345E+15	5.39	6.36	0.075
225	5.852	0.05852	7.573347491	1.33241E+15	5.51	6.46	0.076
220	5.824	0.05824	7.614284835	1.36269E+15	5.64	6.55	0.076
215	5.846	0.05846	7.582086654	1.39438E+15	5.77	6.61	0.076
210	5.911	0.05911	7.488360617	1.42758E+15	5.90	6.65	0.075
205	6.02	0.0602	7.335747841	1.4624E+15	6.05	6.66	0.073
200	6.149	0.06149	7.16214848	1.49896E+15	6.20	6.66	0.072

Table 6: Reflux 2:1 mol ratio

2:1 Zn-TiO2 (Reflux)							
wavelength	% Reflectance	Reflectance	F(R)=(1-R)^2/(2R)	v=c/wavelength	E=hv	sqrt(F(R)*E)	Absorbance
800	105.153	1.05153	0.001262608	3.74741E+14	1.55	0.04	0
795	105.112	1.05112	0.001243081	3.77097E+14	1.56	0.04	0
790	105.063	1.05063	0.001219933	3.79484E+14	1.57	0.04	0
785	105.075	1.05075	0.001225583	3.81901E+14	1.58	0.04	0
780	105.031	1.05031	0.001204928	3.84349E+14	1.59	0.04	0
775	105.006	1.05006	0.001193267	3.86829E+14	1.60	0.04	0
770	104.962	1.04962	0.001172874	3.89341E+14	1.61	0.04	0
765	104.912	1.04912	0.001149904	3.91886E+14	1.62	0.04	0
760	104.878	1.04878	0.001134408	3.94464E+14	1.63	0.04	0
755	104.819	1.04819	0.001107755	3.97076E+14	1.64	0.04	0
750	104.794	1.04794	0.001096553	3.99723E+14	1.65	0.04	0
745	104.816	1.04816	0.001106408	4.02406E+14	1.66	0.04	0
740	104.826	1.04826	0.001110902	4.05125E+14	1.68	0.04	0
735	104.829	1.04829	0.001112251	4.07881E+14	1.69	0.04	0
730	104.799	1.04799	0.001098789	4.10675E+14	1.70	0.04	0
725	104.75	1.0475	0.001076969	4.13507E+14	1.71	0.04	0
720	104.706	1.04706	0.001057553	4.16378E+14	1.72	0.04	0
715	104.697	1.04697	0.001053603	4.1929E+14	1.73	0.04	0
710	104.678	1.04678	0.001045286	4.22243E+14	1.75	0.04	0
705	104.681	1.04681	0.001046597	4.25238E+14	1.76	0.04	0
700	104.695	1.04695	0.001052726	4.28275E+14	1.77	0.04	0
695	104.694	1.04694	0.001052287	4.31356E+14	1.78	0.04	0
690	104.727	1.04727	0.001066799	4.34482E+14	1.80	0.04	0
685	104.773	1.04773	0.001087185	4.37653E+14	1.81	0.04	0
680	104.817	1.04817	0.001106857	4.40871E+14	1.82	0.04	0
675	104.822	1.04822	0.001109103	4.44137E+14	1.84	0.05	0
670	104.814	1.04814	0.001105511	4.47451E+14	1.85	0.05	0
665	104.828	1.04828	0.001111801	4.50816E+14	1.86	0.05	0
660	104.852	1.04852	0.001122625	4.54231E+14	1.88	0.05	0
655	104.893	1.04893	0.001141232	4.57698E+14	1.89	0.05	0
650	104.903	1.04903	0.001145792	4.61219E+14	1.91	0.05	0
645	104.918	1.04918	0.001152649	4.64795E+14	1.92	0.05	0
640	104.935	1.04935	0.001160443	4.68426E+14	1.94	0.05	0
635	104.913	1.04913	0.001150361	4.72114E+14	1.95	0.05	0
630	104.895	1.04895	0.001142143	4.75861E+14	1.97	0.05	0
625	104.854	1.04854	0.00112353	4.79668E+14	1.98	0.05	0
620	104.851	1.04851	0.001122173	4.83536E+14	2.00	0.05	0
615	104.831	1.04831	0.001113152	4.87467E+14	2.02	0.05	0
610	104.793	1.04793	0.001096106	4.91463E+14	2.03	0.05	0
605	104.732	1.04732	0.001069006	4.95525E+14	2.05	0.05	0
600	104.68	1.0468	0.00104616	4.99654E+14	2.07	0.05	0
595	104.639	1.04639	0.001028313	5.03853E+14	2.08	0.05	0
590	104.601	1.04601	0.001011902	5.08123E+14	2.10	0.05	0
585	104.535	1.04535	0.0009837	5.12466E+14	2.12	0.05	0
580	104.453	1.04453	0.000949193	5.16884E+14	2.14	0.05	0
575	104.35	1.0435	0.000906684	5.21378E+14	2.16	0.04	0
570	104.262	1.04262	0.000871106	5.25952E+14	2.18	0.04	0
565	104.185	1.04185	0.000840535	5.30606E+14	2.19	0.04	0
560	104.103	1.04103	0.000808555	5.35344E+14	2.21	0.04	0
555	104.013	1.04013	0.000774142	5.40167E+14	2.23	0.04	0

550	103.88	1.0388	0.000724605	5.45077E+14	2.25	0.04	0
545	103.741	1.03741	0.00067452	5.50078E+14	2.27	0.04	0
540	103.601	1.03601	0.000625824	5.55171E+14	2.30	0.04	0
535	103.497	1.03497	0.000590791	5.6036E+14	2.32	0.04	0
530	103.365	1.03365	0.00054773	5.65646E+14	2.34	0.04	0
525	103.23	1.0323	0.000505323	5.71033E+14	2.36	0.03	0
520	103.091	1.03091	0.000463391	5.76524E+14	2.38	0.03	0
515	102.939	1.02939	0.000419555	5.82121E+14	2.41	0.03	0
510	102.78	1.0278	0.000375968	5.87828E+14	2.43	0.03	0
505	102.599	1.02599	0.000329185	5.93648E+14	2.46	0.03	0
500	102.428	1.02428	0.000287772	5.99585E+14	2.48	0.03	0
495	102.217	1.02217	0.000240424	6.05641E+14	2.50	0.02	0
490	102.013	1.02013	0.00019861	6.11821E+14	2.53	0.02	0
485	101.77	1.0177	0.000153921	6.18129E+14	2.56	0.02	0
480	101.511	1.01511	0.000112457	6.24568E+14	2.58	0.02	0
475	101.224	1.01224	7.4003E-05	6.31142E+14	2.61	0.01	7.397E-07
470	100.885	1.00885	3.88177E-05	6.37856E+14	2.64	0.01	3.882E-07
465	100.497	1.00497	1.22894E-05	6.44715E+14	2.67	0.01	1.231E-07
460	100.053	1.00053	1.40376E-07	6.51723E+14	2.70	0.00	1.425E-09
455	99.538	0.99538	1.07217E-05	6.58885E+14	2.72	0.01	1.074E-07
450	98.94	0.9894	5.67819E-05	6.66205E+14	2.76	0.01	5.683E-07
445	98.232	0.98232	0.000159104	6.73691E+14	2.79	0.02	0
440	97.412	0.97412	0.000343784	6.81346E+14	2.82	0.03	0
435	96.445	0.96445	0.000655193	6.89178E+14	2.85	0.04	0
430	95.322	0.95322	0.001147882	6.97192E+14	2.88	0.06	0
425	93.993	0.93993	0.001919507	7.05394E+14	2.92	0.07	0
420	92.427	0.92427	0.003102466	7.13792E+14	2.95	0.10	0
415	90.559	0.90559	0.004921238	7.22391E+14	2.99	0.12	0
410	88.327	0.88327	0.007713323	7.31201E+14	3.02	0.15	0
405	85.608	0.85608	0.012097565	7.40228E+14	3.06	0.19	0
400	82.175	0.82175	0.01933256	7.49481E+14	3.10	0.24	0
395	77.707	0.77707	0.031977676	7.58968E+14	3.14	0.32	0
390	71.748	0.71748	0.055623537	7.68699E+14	3.18	0.42	0.001
385	64.046	0.64046	0.10091888	7.78682E+14	3.22	0.57	0.001
380	54.869	0.54869	0.185606368	7.88928E+14	3.26	0.78	0.002
375	44.891	0.44891	0.338264004	7.99447E+14	3.31	1.06	0.003
370	35.027	0.35027	0.602605237	8.1025E+14	3.35	1.42	0.006
365	26.175	0.26175	1.041094675	8.21349E+14	3.40	1.88	0.01
360	19.034	0.19034	1.722048218	8.32757E+14	3.44	2.44	0.017
355	14.058	0.14058	2.626983698	8.44486E+14	3.49	3.03	0.026
350	10.915	0.10915	3.635427038	8.56555E+14	3.54	3.59	0.036
345	9.084	0.09084	4.549603179	8.68964E+14	3.59	4.04	0.045
340	7.976	0.07976	5.308686419	8.81743E+14	3.65	4.40	0.053
335	7.385	0.07385	5.807405704	8.94903E+14	3.70	4.64	0.058
330	7.137	0.07137	6.041429711	9.08462E+14	3.76	4.76	0.06
325	7.051	0.07051	6.126447739	9.22438E+14	3.81	4.83	0.061
320	7.034	0.07034	6.143500964	9.36851E+14	3.87	4.88	0.061
315	7.007	0.07007	6.170756421	9.51722E+14	3.94	4.93	0.062
310	7.036	0.07036	6.141490404	9.67072E+14	4.00	4.96	0.061
305	7.13	0.0713	6.048272721	9.82926E+14	4.07	4.96	0.06
300	7.278	0.07278	5.906409236	9.99308E+14	4.13	4.94	0.059
295	7.457	0.07457	5.742394293	1.01625E+15	4.20	4.91	0.057
290	7.613	0.07613	5.605778122	1.03377E+15	4.28	4.90	0.056
285	7.732	0.07732	5.505292178	1.0519E+15	4.35	4.89	0.055
280	7.811	0.07811	5.440284036	1.07069E+15	4.43	4.91	0.054
275	7.863	0.07863	5.398211096	1.09015E+15	4.51	4.93	0.054

270	7.904	0.07904	5.365430931	1.11034E+15	4.59	4.96	0.054
265	7.93	0.0793	5.34482024	1.13129E+15	4.68	5.00	0.053
260	7.919	0.07919	5.353523526	1.15305E+15	4.77	5.05	0.054
255	7.84	0.0784	5.41675102	1.17566E+15	4.86	5.13	0.054
250	7.686	0.07686	5.543764374	1.19917E+15	4.96	5.24	0.055
245	7.475	0.07475	5.726338211	1.22364E+15	5.06	5.38	0.057
240	7.26	0.0726	5.923352342	1.24914E+15	5.17	5.53	0.059
235	7.082	0.07082	6.095562499	1.27571E+15	5.28	5.67	0.061
230	6.95	0.0695	6.228994604	1.30345E+15	5.39	5.79	0.062
225	6.874	0.06874	6.308155278	1.33241E+15	5.51	5.90	0.063
220	6.839	0.06839	6.345205382	1.36269E+15	5.64	5.98	0.063
215	6.83	0.0683	6.354794217	1.39438E+15	5.77	6.05	0.064
210	6.886	0.06886	6.295539498	1.42758E+15	5.90	6.10	0.063
205	6.987	0.06987	6.19108213	1.4624E+15	6.05	6.12	0.062
200	7.231	0.07231	5.950827936	1.49896E+15	6.20	6.07	0.06